Semi-empirical model for shear strength of RC interior beam-column joints subjected to cyclic loads

Margherita Pauletta[a], Caterina Di Marco[b,*], Giada Frappa[a], Giuliana Somma[a], Igino Pitacco[a], Marco Miani[a], Sreekanta Das[c], Gaetano Russo[a]

[a] *Polytechnic Department of Engineering and Architecture, University of Udine, Via delle Scienze 206, 33100 Udine, Italy*
[b] *Polytechnic Department of Engineering and Architecture, University of Udine, Via delle Scienze 206, 33100 Udine, Italy*
[c] *Civil and Environmental Engineering, Faculty of Engineering, University of Windsor, Windsor, Canada*

ARTICLE INFO

Keywords:
Interior beam-column joint
Reinforced concrete
Shear strength
Strut-and-tie model
Test data
Design formula

ABSTRACT

This paper proposes an extension to RC interior beam-column joints of a model for the shear strength prediction of exterior joints under seismic actions, already presented in the literature and based, for certain assumptions, on a previous work of Park and Mosalam. The necessary changes, due to the joints' different physical configurations, only one beam converging in exterior joints and two beams converging in interior ones, are introduced. In the proposed model, on the basis of mechanical considerations, a direct formula for interior joint shear strength accounting for the resisting contributions of three inclined concrete struts and of joint reinforcements, the column horizontal stirrups and intermediate vertical bars, is derived. In comparison to the model for exterior joints, three struts are considered instead of two and the influenced of the upper column axial load on the inclination of the concrete struts is taken into account. The coefficients of the contributions of the struts and reinforcements are calibrated using 69 test data sets available in the literature, selecting only cyclic tests showing joint shear failure. For the validation of the proposed model, the shear strength predictions obtained using the proposed expression are compared with those obtained from Kassem's model, Wang et al.'s formula and Kim and LaFave's formula, on a set of 28 specimens. It is also proposed a design formula, whose predictions are compared to those of Eurocode 8 and ACI Code.

1. Introduction

The main feature of seismic design of beam-column joints in ductile frames is to ensure the complete development of plastic hinges of adjacent elements (ordinarily the beams) and the dissipation of seismic energy, while preventing the occurrence of brittle failure mechanisms during earthquake shaking. Given the importance of shear design of RC beam-column joints, various codes [1,2] and authors [3–16] have tried to predict the strength of these structural elements under seismic loads.

The provisions of Eurocode 8 [1] for the design of interior beam-column connections are based on the strut-and-tie mechanisms, which take into account the contributions of the concrete strut and of both horizontal stirrups and vertical reinforcement of the joint. In ACI Building Code [2] instead, the shear strength for interior beam-column joints design only depends on the geometrical characteristic of the joint and the cylindrical compressive strength of concrete. However, both Codes require that column confinement be continued also in the joint region, assuring confinement to the diagonal strut.

Several authors proposed empirical and mathematical models to evaluate joint shear strength, taking into account the contributions of the concrete, the passing bars within the joint panel and the geometrical and mechanical characteristics of the elements. Kim and LaFave [6] introduced a parametrical simplified formula for joints with horizontal reinforcement, referring to the Bayesian estimation method. Wang et al. [7] proposed a model which included the nominal tensile strength of an idealized plane stressed concrete, the influence of the axial load of the column and the contributions of both the horizontal stirrups and the intermediate vertical bars in the joint core. Kassem [8] proposed an explicit formula by summing the different contributions given by the diagonal concrete strut, the joint stirrups and the column intermediate bars. In other cases, the shear strength calculation is based on an iterative procedure, like those reported by Hwang and Lee [13] or

* Corresponding author.
E-mail addresses: margherita.pauletta@uniud.it (M. Pauletta), dimarco.caterina@spes.uniud.it (C. Di Marco), giada.frappa@uniud.it (G. Frappa), giuliana.somma@uniud.it (G. Somma), igino.pitacco@uniud.it (I. Pitacco), miani.marco.2@spes.uniud.it (M. Miani), sdas@uwindsor.ca (S. Das), gaetano.russo@uniud.it (G. Russo).

Accepted 13 August 2020

Wong and Kuang [16]. Despite all the proposals present in the literature, the resulting values of the joint shear strengths are not always accurate, due to difficulties in accounting for all the mechanisms involved in the behavior of ductile frames' joints.

In this study, a strut-and-tie model is proposed to determine the shear strength of interior joints; it represents an evolution of the models provided by Park and Mosalam [17] and Pauletta et al. [18] for exterior joints without and with shear reinforcement, respectively. In order to identify the forces acting in the joint core and on the cross sections of the adjacent elements, a plane frame joint is considered for simplicity.

The proposed shear strength model considers an approximate constitutive relationship for concrete softening response under plane stress state, based on Hwang and Lee's model [19], eliminating the need for an iterative procedure. Furthermore, the proposed model considers the contributions of three inclined concrete compression struts, horizontal stirrups, and intermediate vertical bars crossing the joint core. The inclination of the concrete struts takes into account the axial load transferred to the joint by the upper column. All contributions are obtained on the basis of mechanical considerations and are multiplied by coefficients, which are derived from a collection of 69 test data found in the literature. The experimental results considered in this study concern interior RC beam-column joints that collapsed due to shear only, under the application of reversal cyclic forces. The collection of test data incorporates also 9 beam-column units without horizontal stirrups.

The accuracy and consistency of the prediction model are evaluated by means of comparison with predictions of the shear strength model proposed by Kim and LaFave [6], the model of Wang et al. [7], and the formula by Kassem [8] on 28 test data, different from the group of tests used for the calibration of the coefficients.

This paper proposes also a design formula, whose predictions are compared to the design and nominal shear strengths obtained from the expressions of Eurocode 8 [1] and ACI Building Code [2], respectively.

2. Model basis

The forces transferred to a typical cruciform interior beam-column joint by the adjacent beams and columns under seismic load conditions are the shear actions and the tensile and compressive forces induced by flexure and axial actions, as shown in Fig. 1(a).

The horizontal shear force acting in the joint core, V_{jh}, can be computed as follows

$$V_{jh} = T + C' - V_{c1} \tag{1}$$

where T is the tensile force in the top beam longitudinal bars, C' is the compression force in the beam section on the opposite side of the joint and V_{c1} the horizontal shear force acting in the column above the joint.

Therefore

$$T = A_{sb1} f_{b1} \tag{2}$$

where A_{sb1} and f_{b1} are the transverse area and the tensile stress in the beam top reinforcement respectively, $C' = C_s^{'} + C_c^{'}$, with $C_s^{'}$ the compression force in the top beam longitudinal bars (on the opposite side of the joint) and $C_c^{'}$ the compression force acting on the concrete in the beam section.

Applying the horizontal equilibrium equation to the beam cross section gives $C' = T^{'}$, where

$$T^{'} = A_{sb2} f_{b2} \tag{3}$$

with A_{sb2} and f_{b2} the transverse area and the tensile stress in the beam bottom reinforcement, respectively.

Thus the value of $C_s^{'}$ can be calculated as difference between $T^{'}$ and $C_c^{'}$ as follows

$$C_s^{'} = T^{'} - C_c^{'} \tag{4}$$

By adopting, in the beam cross section, a linear stress distribution (Fig. 1(b)I) or a stress block (Fig. 1(b)II) distribution, $C_c^{'}$ can be computed by means of the following expressions, respectively

$$C_c^{'} = \frac{1}{2} \bullet \sigma_c x_{b2} b_b \tag{5}$$

$$C_c^{'} = 0.8 \bullet x_{b2} b_b f_c^{'} \tag{6}$$

where σ_c is the maximum concrete compression stress in the beam cross section for the linear distribution, x_{b2} is the neutral axis depth, and b_b is the beam width (Fig. 1(b)). The value of x_{b2} can be computed from the horizontal equilibrium of the beam internal forces.

3. Joint shear strength

The horizontal shear nominal strength of interior RC beam-column joints V_n is obtained by adding two resisting contributions associated with two coexisting mechanisms of shear transfer [17]

$$V_n = V_{hc} + V_{hs} \tag{7}$$

where V_{hc} is the resisting contribution of concrete, provided by the principal strut ST1 ($V_{hc,ST1}$) and two side inclined struts ST2 and ST3 ($V_{hc,ST2-3}$) shown in Fig. 2(a), which can be expressed as follows

$$V_{hc} = V_{hc,ST1} + V_{hc,ST2-3} \tag{8}$$

and V_{hs} is the resisting contribution given by the truss mechanism, induced by the horizontal stirrups and the vertical reinforcement of the joint core (Fig. 3).

Hence, the sum of contributions shown in Figs. 2(a) and 3 give the total shear strength of the interior beam-column joint.

It has to be observed that the difference introduced in the model for interior joints respect to the model for exterior ones [18] is the presence of three concrete struts instead of two (Fig. 2(b)).

In the exterior joint in Fig. 2(b) the strut ST2 arises from the transfer to the joint core of a fraction of the beam top reinforcement tensile force, by means of bond. Contrariwise, it is assumed that the bond stresses transferred by the beam bottom reinforcement are negligible,

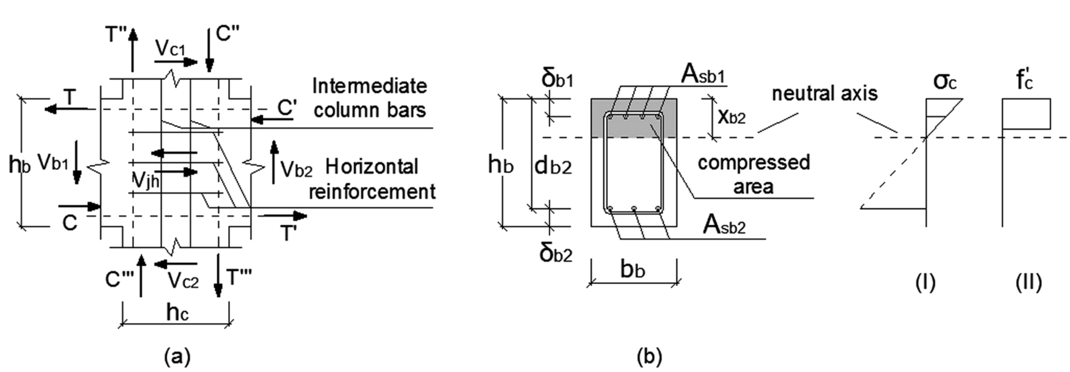

Fig. 1. (a) External actions on the interior beam-column joint core in seismic conditions; (b) right beam section: I linear stress distribution, II stress-block distribution.

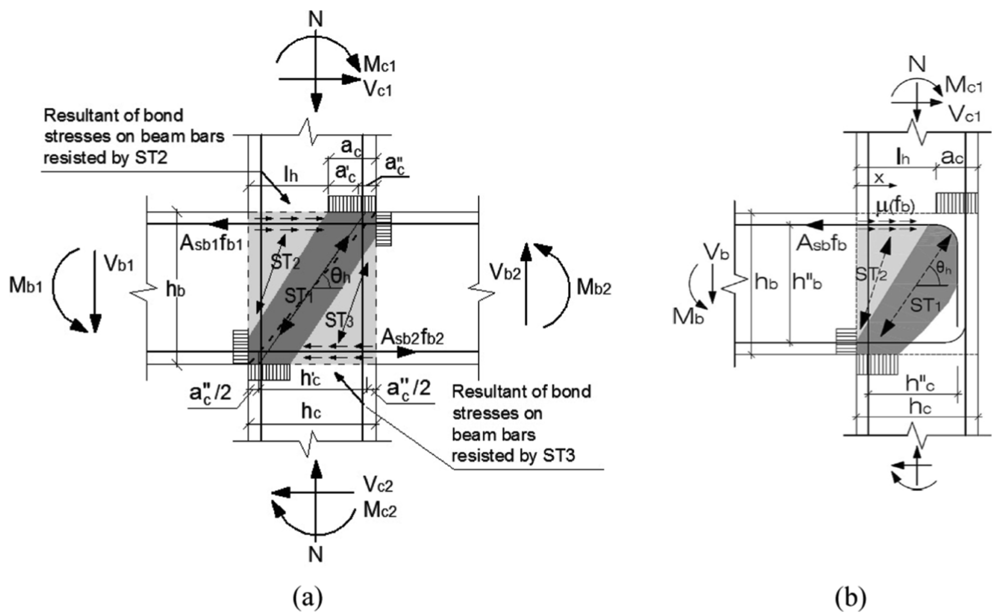

Fig. 2. The concrete struts: (a) three in interior joints; (b) two in exterior ones [18].

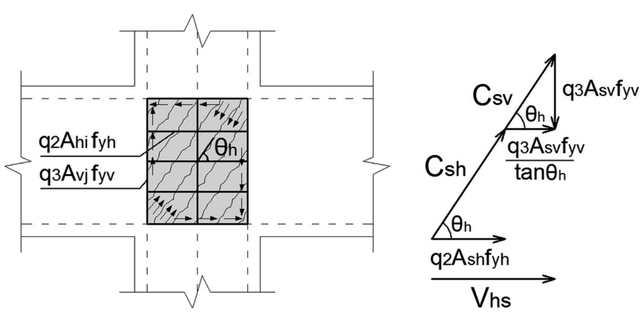

Fig. 3. Truss mechanism contributions.

because this reinforcement is subjected to a compressive lower intensity force.

In the interior joint in Fig. 2(a), the strut ST2 arises similarly to exterior joints, but also strut ST3 is present due to the transfer of bond stresses from the beam bottom reinforcement, which, in the region relevant to strut ST3, is subjected to a high tensile force inducing not negligible bond stresses.

In the proposed model it is assumed that joint shear failure is caused by the crushing of the main strut ST1, confined by any horizontal stirrup and vertical reinforcement in the joint core. The development of the inclined strut is marked by the onset of inclined cracks within the joint panel. Cases of failure due to bond deterioration inside the joint are not considered in this research.

The proposed model assumes that a fraction β, with $0 \le \beta \le 1$, of the total horizontal force $T + C_s^{'}$ (Fig. 2(a)) transferred from the top beam longitudinal reinforcement to the concrete, by means of bond, is supported by the inclined struts ST2-3, and that the remaining rate $(1-\beta)\bullet(T + C_s^{'})$ is transferred to the two trusses induced in the joint core by steel vertical and horizontal (stirrups) joint reinforcement (Fig. 3).

Thus, the rate of V_{jh} transferred to the truss mechanism only by bond, $V_{jh,s}$, can be expressed as follows [21]

$$V_{jh,s} = (1-\beta)\bullet(T + C_s^{'}) \tag{9}$$

The residual rate of V_{jh} transferred to the concrete inclined struts, $V_{jh,c}$, can be derived from Eq. (1)

$$V_{jh,c} = \beta(T + C_s^{'}) + C_c^{'} - V_{c1} \tag{10}$$

At joint failure the horizontal shear force in the joint core equals the joint strength

$$V_{jh} = V_n \tag{11}$$

3.1. Contribution of strut mechanisms to joint shear strength V_{hc}

Park and Mosalam's model [17] considers exterior beam-column joints without both stirrups inside the joint core and vertical intermediate column bars crossing it, and it assumes that the horizontal resisting mechanisms that develop in the joint core is given by two inclined and parallel concrete struts, ST1 and ST2. More specifically, ST1 is the strut that is activated when the 90-degree hooked beam reinforcement anchored inside the joint is subjected to tensile stresses, hence it transfers diagonal compressive stresses inside the joint core, and ST2 is the strut arising from the transfer to the joint core of a fraction of the beam reinforcement tensile force, by means of bond. For the development of these mechanisms, bond failure of the beam reinforcement anchorage have to be avoided.

With reference to Fig. 2(a), in the proposed model it is assumed that ST1 is the strut developed by beam and column flexural compression zones and a fraction of the beam longitudinal bars force, transferred by bond along the bar portion contained within the dark shaded region in Fig. 2(a). The inclined strut ST2, assumed to be parallel to ST1, is developed by bond forces transferred to the joint core by the beam top bars along the clear shaded region in Fig. 2(a) (length l_h). The strut ST3, parallel to ST1 and ST2, forms in the other side of the joint region due to the bond forces transferred to the joint core by the beam bottom bars. The three struts' configuration is inverted at the inversion of the acting seismic forces.

3.1.1. Shear strength contribution $V_{hc,sT1}$

The contribution to joint shear strength of the main concrete strut ST1 ($V_{hc,ST1}$) is evaluated considering that the depth of the strut is equal to the depth of the column flexural compression zone a_c (Fig. 2(a)), whose value can be approximated by [21]

$$a_c = \left(0.25 + 0.85\frac{N}{A_g f_c^{'}}\right) h_c \tag{12}$$

where N is the compression force in the column above the joint, $f_c^{'}$ is

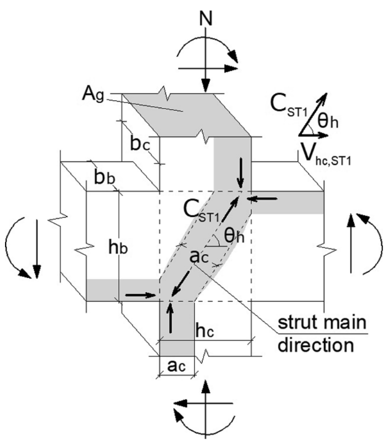

Fig. 4. Inclined strut ST1 mechanism contribution.

the cylindrical compressive strength of concrete and A_g (Fig. 4) is the area of the whole column cross section.

By decomposing a_c into its two components (Fig. 2(a))

$$a_c^{'} = 0.25h_c \tag{13}$$

which is independent from the column axial load N, and

$$a_c'' = 0.85\frac{N}{A_g f_c'}h_c \tag{14}$$

which, instead, is function of N, Eq. (12) can be written as follows

$$a_c = a_c^{'} + a_c^{''} \tag{15}$$

The inclination angle θ_h of the inclined struts ST1, ST2 and ST3 is defined by

$$\theta_h = \tan^{-1}\left(\frac{h_b}{h_c^{'}}\right) \tag{16}$$

where it is assumed that, when $N = 0$, $h'_c = h_c$, while, when $N > 0$, a reorientation of the strut ST1 arises due to the presence of the additional length rate a'_c in a_c. This reorientation occurs so that the end of the strut is centered on half the length a'_c (Fig. 2(a)), hence $h_c$is given by the following equation (Fig. 2(a))

$$h_c^{'} = h_c - a_c^{''} \tag{17}$$

The width b_j of the inclined strut ST1 is expressed [1] as (Fig. 4)

$$b_j = \begin{cases} \min(b_c,\, b_b + 0.5h_c) & \text{for} \quad b_b < b_c \\ \min(b_b,\, b_c + 0.5h_c) & \text{for} \quad b_b \geq b_c \end{cases} \tag{18}$$

Naming $C_{ST1,max}$ the maximum compression force (parallel to the strut ST1) that the strut ST1 can sustain, in accordance with the strut-and-tie model, the horizontal shear strength of strut ST1 can be expressed as follows

$$V_{hc,sT1,max} = C_{ST1,max}\bullet\cos\theta_h \tag{19}$$

where θ_h, defined by Eq. (16), is the inclination angle of the strut ST1 with respect to the horizontal direction.

The cross-sectional area of the inclined main concrete strut ST1 is considered [19] equal to $a_c\bullet b_j$ (Fig. 4), and its principal axis of inertia are assumed respectively parallel and orthogonal to the direction of its inclination.

In the presence of the transverse tensile strain ε_r, the maximum compression stress (< 0) that may develop in the strut principal direction is given by [19]

$$\sigma_{d,max} = -\zeta\bullet f_c^{'} \tag{20}$$

where

$$\zeta = \frac{5.8}{\sqrt{f_c^{'}}}\frac{1}{\sqrt{1+400\varepsilon_r}} \leq \frac{0.9}{\sqrt{1+400\varepsilon_r}} \tag{21}$$

Hence, the maximum compression force $C_{ST1,max}$, acting in the main concrete strut, is

$$C_{ST1,max} = -\sigma_{d,max}\, a_c b_j \tag{22}$$

Eq. (21) is verified if $5.8/\sqrt{f_c^{'}[\text{MPa}]} \leq 0.9$, that is $f_c^{'} \geq 42$ MPa, and, in this case, ζ assumes the value given by the left member of the inequality. Otherwise, ζ is equal to the right member of the inequality.

To gain the expression of ε_r to be used in Eq. (21) the constitutive law of tensile concrete can be considered linear with constant slope up to the ultimate tensile strength and, within this range, it can be assumed that the tensile Young's modulus is equal to that in compression. It results that ε_r can be expressed as $\varepsilon_r = \sigma_t/E_c$, where σ_t is the transverse stress in the concrete strut ST1 at joint failure.

The inclined concrete strut ST1 is subjected to a biaxial tension-–compression stress state, which is unknown, because the maximum compressive and tensile stresses at failure, $\sigma_{d,max}$ and σ_t, are not known a priori.

It is known that concrete tensile strength in a biaxial tension-–compression regime is lower than that under uniaxial regime. For this reason, the maximum value of tensile stress $\sigma_{t,lim}$ can be assumed equal to the limit value f_{ct} of concrete tensile strength and, for a safe computation, Eq. (20) can be expressed as $\sigma_{d,lim} = \sigma_{d,max|\varepsilon_r = f_{ct}/E_c}$.

To hold a single expression for $\sigma_{d,lim}$, the following approximation [22,23] depending on $f_c^{'}$ is used

$$\sigma_{d,lim}^{*} = -\chi f_c^{'} \tag{23}$$

where χ is a non-dimensional interpolating function ([22,23]), also depending only on $f_c^{'}$, expressed as

$$\chi = 0.74\bullet\left(\frac{f_c^{'}}{105}\right)^3 - 1.28\bullet\left(\frac{f_c^{'}}{105}\right)^2 + 0.22\bullet\left(\frac{f_c^{'}}{105}\right) + 0.87 \tag{24}$$

with the limit range for the cylindrical compressive strength of $10 \leq f_c^{'} \leq 105\text{MPa}$. This equation is valid in general independently from the type of RC member [22].

Consequently, the approximating limiting value of the main concrete strut's shear contribution $V_{hc,ST1,lim}^{*}$ is obtained by substituting Eq. (22) in Eq. (19), and it is given by

$$V_{hc,ST1,lim}^{*} = \chi f_c^{'}\bullet a_c\bullet b_j\bullet\cos\theta_h \tag{25}$$

Since $V_{hc,ST1,lim}^{*}$ is obtained by approximating $V_{hc,sT1,max}$ and the compression stress in the strut ST1 at joint failure will be lower or eventually equal to the maximum compression concrete strength $\sigma_{d,lim}^{*}$, it follows that the horizontal shear strength contribution of strut ST1 $V_{hc,ST1}$ (Fig. 4) can be expressed as follows

$$V_{hc,ST1} = q_1\bullet\chi f_c^{'}\bullet a_c\bullet b_j\bullet\cos\theta_h \tag{26}$$

where q_1 is a positive factor ($0 \leq q_1 \leq 1$), whose value is derived on the basis of experimental results.

3.1.2. *Shear strength contribution $V_{hc,sT2-3}$*

The ST2 strut contribution to the horizontal joint shear strength, as noted above, is developed by bond forces transferred to the joint core by the beam top bars along the clear shaded region in Fig. 2(a).

When joint shear failure occurs, the horizontal contribution of the concrete strut ST2 to the joint shear strength can be expressed as

$$V_{hc,ST2} = \beta\sum_{i=0}^{s} n_{b1,i}\bullet\pi\bullet\Phi_{b1,i}\int_0^{l_h}\mu(f_{b1})dx \tag{27}$$

where s is the number of different bar diameters present at the beam top; $\mu(f_b)$ represents the local bond stress of beam reinforcement, which, in real conditions, varies with the distance from the beam-column interface, and it is a function of the tensile stress acting in the beam top bars, f_{b1}; $n_{b1,i}$ is the number of top beam longitudinal bars (in tension) with corresponding diameter $\Phi_{b1,i}$; and l_h is the depth of the concrete strut ST2, which derives from

$$l_h = h_c - a_c \tag{28}$$

The ST3 strut contribution to the horizontal joint shear strength has an expression similar to Eq. (27), that is

$$V_{hc,ST3} = \beta \sum_{i=0}^{t} n_{b2,i} \bullet \pi \bullet \Phi_{b2,i} \int_0^{l_h} \mu(f_{b2}) dx \tag{29}$$

where t is the number of different bar diameters present at the beam bottom.

Since the variable bond stress distribution is unknown and would be too burdensome to handle, it is possible, referring to expressions available in the literature [24–26], to assume an approximate uniform value of bond stress, $\bar{\tau}$, along the joint portion l_h, both at the top and at the bottom of the beam, that is

$$\mu(f_{b1}) = \mu(f_{b2}) = \bar{\tau} \tag{30}$$

By substituting Eq. (30) in Eq. (27) and in Eq. (29) and, subsequently, simplifying them by introducing the average diameters Φ_{b1} and Φ_{b2} of the top and bottom beam longitudinal bars, respectively, the sum of the contribution of the side inclined struts ST2 and ST3 can be written as follows

$$V_{hc,ST2-3} = \beta(n_{b1}\Phi_{b1} + n_{b2}\Phi_{b2})\pi l_h \bar{\tau} \tag{31}$$

where n_{b1} and n_{b2} are the number of the top and bottom beam longitudinal bars, respectively, with corresponding average diameters Φ_{b1} and Φ_{b2}, calculated on the basis of the top and bottom beam reinforcements A_{sb1} and A_{sb2}, and the fraction factor β is determined on the basis of experimental results.

3.2. Reinforcement contribution to joint shear strength $\mathbf{V_{hs}}$

Beam-column joints can be reinforced by m levels of n-leg horizontal stirrups and p intermediate vertical column bars. The i-th stirrup level has cross-sectional area A_{hi} ($i = 1, \ldots, m$), while the j-the vertical bar has cross-sectional area A_{vj} ($j = 1, \ldots, p$). For the steel reinforcement contribution to joint shear strength, only the horizontal stirrups and vertical bars within the effective joint area $h_c \bullet b_j$ are considered in this model.

When both horizontal stirrups and vertical joint reinforcement bars are present, two strut-and-tie mechanisms (one due to the stirrups and one due to the vertical bars) form within the joint core, that work independently each other and contribute by super-position (Fig. 3) to the overall truss shear strength [19].

It is assumed herein (Fig. 3) that in the truss mechanisms the inclined compression resultants C_{sh} and C_{sv}, related to the horizontal stirrups and vertical reinforcement, respectively, are parallel to the three inclined concrete struts ST1, ST2 and ST3, and, for this reason, their contributions are added each other.

Russo et al. [18,22–23] observed that, for exterior joints, corbels and deep beams, not all the horizontal reinforcements undergo to yielding in the condition of shear failure: the mid-height bars reach the yield strength f_{yh}, while other levels may be subjected to lower stresses. Similarly, the vertical bars probably reach the yield strength f_{yv} in the central region, whereas they achieve lower tensions elsewhere. This observation is considered valid also for the horizontal stirrups and vertical intermediate bars of interior beam-column joints.

Hence, the mean stress in the horizontal stirrups can be expressed as $q_2 f_{yh}$, with $0 < q_2 < 1$, and the mean stress in the vertical bars as $q_3 f_{yv}$, with $0 < q_3 < 1$. As a consequence, the horizontal force provided by the stirrups results $q_2 A_{sh} f_{yh}$, and the vertical force provided by the intermediate column bars is equal to $q_3 A_{sv} f_{yv}$ (Fig. 3), with

$$A_{sh} = \sum_{i=0}^{m} A_{hi}$$
$$A_{sv} = \sum_{i=0}^{p} A_{vi} \tag{32}$$

Thus, the contribution to shear strength, V_{hs}, provide by steel reinforcements, is equal to the vector sum (Fig. 3) of the horizontal force provided by the horizontal stirrups, $q_2 A_{sh} f_{yh}$, and the horizontal component of the resultant of compression forces acting in the inclined struts in the truss mechanism induced by the intermediate column bars, $q_3 A_{vj} f_{yv}/\tan\theta_h$

$$V_{hs} = q_2 A_{sh} f_{yh} + q_3 A_{sv} f_{yv}/\tan\theta_h \tag{33}$$

In the case of beam-column connections without vertical reinforcement, the shear strength contribution Vhs is given only by the horizontal stirrups contribution

$$V_{hs} = q_2 A_{sh} f_{yh} \tag{34}$$

3.3. Shear strength expression

The nominal shear strength formula for interior RC beam-column joints is obtained by introducing Eqs. (26), (31), (8) and (33) in Eq. (7)

$$V_n = 4\beta\left(\frac{A_{sb1}}{\Phi_{b1}} + \frac{A_{sb2}}{\Phi_{b2}}\right) l_h \bar{\tau} + q_1 \chi f_c^{'} a_c b_j \cos\theta_h + q_2 A_{sh} f_{yh} + q_3 \frac{A_{sv} f_{yv}}{\tan\theta_h} \tag{35}$$

where χ and θ_h are respectively expressed by Eqs. (24) and (16), while β, $\bar{\tau}$ q_1, q_2 and q_3 are unknown coefficients, which can be calibrated on the basis of tests' data processing.

In the first term of Eq. (35) it is more convenient to have a unique coefficient to be calibrated, hence it is assumed β $\bar{\tau}$ = q_0 and Eq. (35) becomes

$$V_n = 4q_0\left(\frac{A_{sb1}}{\Phi_{b1}} + \frac{A_{sb2}}{\Phi_{b2}}\right) l_h + q_1 \chi f_c^{'} a_c b_j \cos\theta_h + q_2 A_{sh} f_{yh} + q_3 \frac{A_{sv} f_{yv}}{\tan\theta_h} \tag{36}$$

To determine the parameters$\boldsymbol{q}_0$, $\boldsymbol{q}_1$, $\boldsymbol{q}_2$ and $\boldsymbol{q}_3$, 69 test units have been selected from 25 investigations [28–60]. The original labels of the selected test units are reported in Tables 1 and 2, at the second column. All the considered specimens were cyclically loaded.

In selecting the test data, only interior beam-column joints that exhibited shear failure and not flexural or bond failure were considered.

A set of geometrical and mechanical properties of the specimens are involved to evaluate the joint shear strength with Eq. (35), and the validity ranges resulting from the processing of the collected data are reported in the list below:

- 19.3 MPa $\leq f_c^{'} \leq$ 98.8 MPa;
- 36.9 deg $\leq \theta_h \leq$ 66.7 deg;
- 0 mm^2 $\leq A_{sh} \leq$ 3879.6 mm^2;
- 0 mm^2 $\leq A_{sv} \leq$ 6036.5 mm^2;
- 0 mm^2 $\leq \frac{A_{sv}}{\tan\theta_h} \leq$ 4011 mm^2;
- 235.4 MPa $\leq f_{yb1} \leq$ 1456 MPa;
- 235.4 MPa $\leq f_{yb2} \leq$ 1456 MPa;
- 235.4 MPa $\leq f_{yh} \leq$ 1456 MPa;
- 325 MPa $\leq f_{yv} \leq$ 1456 MPa;
- 0 $\leq \frac{N}{A_g f_c^{'}} \leq$ 0.48;
- Percentage of top flexural reinforcement in the beam: 0.54% $\leq \rho_{sb1} \leq$ 3.59%;
- Percentage of bottom flexural reinforcement in the beam: 0.46% $\leq \rho_{sb2} \leq$ 2.79%.

The coefficient q_1 in Eq. (35) is collected as a common factor, hence Eq. (35) becomes

Table 1
Geometrical properties and reinforcement areas of the 69 specimens used for the calibration of the coefficients $\boldsymbol{q}_0$, $\boldsymbol{q}_1$, $\boldsymbol{q}_2$ and $\boldsymbol{q}_3$ in the proposed formula (Eq. (38)).

Author references	Specimen labels	b_b(mm)	h_b(mm)	b_c(mm)	h_c(mm)	δ_{b1}(mm)	δ_{b2}(mm)	δ_c(mm)	A_{sb1}(mm^2)	A_{sb2}(mm^2)	ϕ_1(mm)	ϕ_2(mm)	A_{sh}(mm^2)	A_{sv}(mm^2)
[28]	E0.0 [a]	250	300	300	300	28	28	28	804	804	16.0	16.0	0	1206
	E0.3 [a]	250	300	300	300	28	28	28	804	804	16.0	16.0	0	1206
	H0.0	250	300	300	300	28	28	28	804	804	16.0	16.0	1017	1206
	H0.3	250	300	300	300	28	28	28	804	804	16.0	16.0	1017	1206
[29]	B1	356	610	457	457	68	68	42	2512	2512	20.0	20.0	2026	452
	B2 [b]	356	610	457	457	68	68	42	2512	2512	20.0	20.0	531	452
[31]	A1	160	250	220	220	38	38	30	570	570	9.5	9.5	170	759
	A2	160	250	220	220	38	38	30	570	570	9.5	9.5	170	759
	A3	160	250	220	220	38	38	30	570	570	9.5	9.5	170	759
[32]	J-HH [b]	200	350	300	300	35	35	30	1519	1519	25.4	25.4	1357	1130
	J-HO [b]	200	350	300	300	35	35	30	1519	1519	25.4	25.4	1357	0
	J-OH [a]	200	350	300	300	35	35	30	1519	1519	25.4	25.4	0	1130
	J-MM [b]	200	350	300	300	35	35	30	1519	1519	25.4	25.4	678	565
	J-MO [b]	200	350	300	300	35	35	30	1519	1519	25.4	25.4	678	0
	J-LO [b]	200	350	300	300	35	35	30	1519	1519	25.4	25.4	28	0
[33]	O1 [a]	300	500	460	300	58	58	58	1809	904	24.0	24.0	0	0
[37]	JXO-B1	150	350	300	300	30	30	30	380	380	12.7	12.7	190	253
[38]	A-1	200	300	300	300	50	50	50	1163	1163	22.2	22.2	509	0
[39]	I3	200	300	300	300	55	40	40	1194	796	15.9	15.9	254	1194
	I5	200	300	300	300	53	53	40	762	381	12.7	12.7	285	1194
	I6	200	300	300	300	40	40	40	861	574	19.1	19.1	285	1194
[40]	B1	200	300	300	300	62	62	40	1016	1016	12.7	12.7	225	1194
	B3	200	300	300	300	62	62	40	856	856	9.5	9.5	592	762
	A1	200	300	300	300	62	40	40	1016	508	12.7	12.7	255	1194
[41]	JE-0	180	300	320	280	51	51	33	710	710	9.5	9.5	192	508
[42]	JI0	300	600	400	400	50	50	50	1519	1519	25.4	25.4	1013	1013
[45]	JA [b]	250	500	400	400	45	30	30	2065	1548	25.4	25.4	1936	1032
	JB [b]	250	500	400	400	45	30	30	2581	1936	19.1	19.1	2439	1032
	JC [b]	230	460	400	400	30	30	30	1548	1548	19.1	19.1	3067	2065
	JD [b]	230	460	400	400	30	30	30	1548	1548	19.1	19.1	3880	2065
[46]	I [b]	279	457	330	457	67	64	62	2457	1519	32.3	25.4	506	1548
	II	279	457	330	457	67	64	67	2457	1519	32.3	25.4	506	3276
	III [b]	279	457	330	457	67	64	69	2457	1519	32.3	25.4	506	6037
	IV [b]	406	457	457	330	67	64	65	2457	1519	32.3	25.4	1013	1266
	V	279	457	330	457	67	64	67	2457	1519	32.3	25.4	506	3276
	VI [b]	279	457	330	457	67	64	67	2457	1519	32.3	25.4	506	3276
	VII [b]	406	457	457	330	67	64	65	2457	1519	32.3	25.4	1013	1266
	XII [b]	279	457	330	457	67	64	67	2457	1519	32.3	25.4	2382	3276
	XIII	279	457	330	457	67	64	67	2457	1519	32.3	25.4	1519	3276
	XIV [b]	406	457	457	330	67	64	67	2457	1519	32.3	25.4	3038	1266
[48]	OKJ-1	200	300	300	300	48	41	40	1194	929	13.0	13.0	339	1061
	OKJ-4	200	300	300	300	48	41	40	1194	929	13.0	13.0	339	1061
[49]	NO.2	200	300	300	300	46	46	37	785	785	10.0	10.0	57	796
	NO.4	200	300	300	300	33	33	37	663	663	13.0	13.0	57	796
[50]	J-1	240	300	300	300	48	41	30	1143	889	12.7	12.7	283	1064
	J-3	240	300	300	300	50	50	30	1064	1064	13.0	13.0	1944	1064
	J-4	240	300	300	300	50	50	30	1266	1266	12.7	12.7	283	1064
	J-5	240	300	300	300	48	41	30	1143	889	12.7	12.7	283	1064
	J-6	240	300	300	300	48	41	30	1143	889	12.7	12.7	170	1064
	J-8	240	300	300	300	48	41	30	2583	2009	19.1	19.1	283	2296
	J-10	240	300	300	300	48	41	30	1143	889	12.7	12.7	283	1064
	J-11	240	300	300	300	48	41	30	2583	2009	19.1	19.1	283	2296
[52]	JO-1	150	150	150	150	20	20	20	381	381	13.0	13.0	113	252
[53]	J0C-1	120	150	150	150	22	22	22	214	214	9.5	9.5	79	0
[54]	1	229	457	305	406	56	56	42	1608	1608	16.0	16.0	3215	904
[55]	1	229	457	305	406	56	56	40	1608	1608	16.0	16.0	2010	628
[56]	1 [a]	356	610	406	406	62	62	64	2564	1282	28.6	28.6	0	0
	2 [a]	356	610	406	406	62	62	64	2564	1282	28.6	28.6	0	0
	3 [a]	356	610	406	406	62	62	60	2564	1282	28.6	28.6	0	0
	4 [b]	356	610	406	406	62	62	59	2564	1282	28.6	28.6	142	776
	5 [b]	356	610	406	406	62	62	59	2564	1282	28.6	28.6	427	776
[57]	S3	200	300	300	300	49	49	35	995	995	16.0	16.0	256	1148
[58]	J3B	175	300	200	350	52	39	30	678	452	12.0	12.0	628	904
[59]	Ho-JI1 [a]	300	400	400	400	40	40	40	1140	1140	19.1	19.1	0	1013
	Ko-JI1 [a]	300	500	300	300	50	50	35	2026	2026	25.4	25.4	0	1013
[60]	BL1	350	500	400	400	38	38	38	1407	1206	16.0	16.0	1809	402
	BL2 [b]	300	500	400	400	52	40	40	1884	1256	20.0	20.0	2035	628
	BL3	250	400	350	450	54	36	36	1608	804	16.0	16.0	1356	402
	BL4	300	500	400	400	47	38	38	1608	1005	16.0	16.0	2035	402

[a] Joints without horizontal hoops.
[b] Joints that did not satisfy both ACI Code and EC8 requirements.

Table 2
Mechanical properties, forces and results of the 69 specimens used for the calibration of the coefficients q_0, q_1, q_2 and q_3 in the proposed formula (Eq. (38)).

Author references	Specimen labels	$f_c^{'}$(MPa)	f_{yh}(MPa)	f_{yv}(MPa)	N(kN)	θ_h(deg)	$V_{hc,ST1}$(%)	$V_{hc,ST2-3}$(%)	$V_{hs,h}$(%)	$V_{hs,v}$(%)	V_n(kN)	$V_{jh,test}$(kN)	$\frac{V_{jh,test}}{V_n}$	$\frac{V_{jh,test}}{V_{n,Kim}}$	$\frac{V_{jh,test}}{V_{n,Wang}}$	$\frac{V_{jh,test}}{V_{n,Kassem}}$	V_d(kN)	$\frac{V_{jh,test}}{V_d}$	$\frac{V_{jh,test}}{V_{d,EC8}}$	$\frac{V_{jh,test}}{V_{d,ACI}}$
[28]	E0.0[a]	43.1	460	513	0	45	63	17	0	20	689	750	1.09	–	–	–	551	1.36	–	–
	E0.3 [a]	46.1	460	558	1080	52	79	9	0	12	947	815	0.86	–	–	–	758	1.08	–	–
	H0.0	50.6	460	595	0	45	59	14	8	19	828	869	1.05	0.89	1.07	0.92	662	1.31	0.84	1.40
	H0.3	45.1	460	518	1080	52	75	8	6	11	994	744	0.75	0.82	0.66	0.80	795	0.94	3.58	1.27
[29]	B1	27.9	346	427	311	54	55	35	8	2	1232	1217	0.99	0.89	1.21	0.96	986	1.23	1.09	1.17
	B2 [b]	31.5	398	427	2890	65	81	16	2	1	1444	1213	0.84	1.03	0.76	0.93	1155	1.05	–	–
[31]	A1	40.2	291	644	162	51	57	21	2	20	443	412	0.93	0.89	1.03	0.49	354	1.16	1.24	1.47
	A2	40.2	291	388	162	51	62	23	2	13	408	380	0.93	1.09	1.12	1.01	326	1.16	1.15	1.35
	A3	40.2	291	644	480	55	68	16	1	15	485	412	0.85	0.89	0.83	0.47	388	1.06	3.05	1.47
[32]	J-HH [b]	32.1	382	578	867	57	67	12	9	12	780	725	0.93	0.83	0.82	0.63	624	1.16	–	–
	J-HO [b]	32.1	382	578	867	57	76	14	10	0	689	696	1.01	0.80	0.95	0.62	551	1.26	–	–
	J-OH [a]	32.1	382	578	867	57	74	13	0	13	709	642	0.91	–	–	–	568	1.13	–	–
	J-MM [b]	32.1	382	578	867	57	75	13	5	7	699	736	1.05	0.94	1.00	0.71	559	1.32	–	–
	J-MO [b]	32.1	382	578	867	57	80	14	5	0	654	752	1.15	0.96	1.15	0.74	523	1.44	–	–
	J-LO [b]	32.1	382	578	867	57	85	15	0	0	620	751	1.21	1.54	1.30	0.81	496	1.51	–	–
[33]	O1 [a]	41.0	0	325	0	59	77	23	0	0	591	527	0.89	–	–	–	473	1.12	–	–
[37]	JXO-B1	21.3	307	371	307	53	79	15	2	4	386	282	0.73	0.80	0.77	1.05	309	0.91	1.37	1.07
[38]	A-1	19.3	324	356	353	50	73	22	5	0	443	495	1.12	0.84	1.24	0.76	355	1.40	6.34	1.42
[39]	I3	41.4	360	361	95	46	65	21	2	13	702	709	1.01	1.09	1.28	1.18	562	1.26	0.97	1.39
	I5	85.4	250	534	177	46	73	11	1	14	944	893	0.95	1.08	1.08	1.17	755	1.18	0.66	1.22
	I6	85.4	250	534	177	46	75	9	1	15	927	1005	1.08	1.13	1.22	1.11	741	1.36	0.75	1.37
[40]	B1	24.5	235	351	176	47	55	29	1	14	593	570	0.96	1.26	1.20	1.37	475	1.20	1.70	1.45
	B3	24.5	235	371	176	47	55	32	3	10	599	515	0.86	0.94	1.13	1.05	479	1.07	1.53	1.31
	A1	30.6	320	539	176	47	58	20	2	20	663	689	1.04	1.01	1.15	0.77	531	1.30	1.45	1.57
[41]	JE-0	27.0	364	345	0	47	57	34	2	7	492	477	0.97	1.00	1.43	1.17	393	1.21	0.99	1.55
[42]	JI0	27.0	456	456	821	61	69	17	7	7	858	876	1.02	0.86	0.95	0.77	687	1.28	2.00	1.14
[45]	JA [b]	33.7	484	484	1618	59	73	12	10	5	1266	1310	1.03	0.93	0.92	0.79	1013	1.29	–	–
	JB [b]	34.8	484	484	1670	59	67	17	11	5	1424	1331	0.93	0.85	0.88	0.66	1139	1.17	–	–
	JC [b]	32.5	461	484	1560	57	65	12	13	10	1455	1359	0.93	0.93	0.81	0.78	1164	1.17	–	–
	JD [b]	33.1	466	484	1589	57	63	11	16	9	1524	1491	0.98	0.98	0.83	0.78	1219	1.22	–	–
[46]	I [b]	26.2	409	457	1588	57	77	12	2	9	1141	1090	0.96	0.97	0.84	0.77	913	1.19	–	–
	II	41.8	409	449	1601	52	72	11	2	16	1612	1597	0.99	1.23	0.92	1.05	1289	1.24	4.22	1.68
	III [b]	26.6	409	402	1584	56	63	10	2	25	1402	1228	0.88	1.09	0.73	0.80	1122	1.09	–	–
	IV [b]	36.0	409	438	1615	62	78	11	5	6	1091	1455	1.33	1.22	1.20	1.02	873	1.67	–	–
	V	35.9	409	449	214	46	55	18	2	24	1275	1530	1.20	1.24	1.28	1.10	1020	1.50	1.56	1.73
	VI [b]	36.8	409	449	2682	60	79	7	2	12	1545	1646	1.07	1.32	0.81	1.04	1236	1.33	–	–
	VII [b]	37.2	409	438	2656	67	83	7	5	5	1138	1468	1.29	1.22	0.99	0.98	910	1.61	–	–
	XII [b]	35.2	423	449	1615	53	66	10	9	15	1595	1948	1.22	1.25	1.05	1.05	1276	1.53	–	–
	XIII	41.3	409	449	1570	52	69	11	5	15	1656	1557	0.94	1.02	0.85	0.92	1325	1.18	4.04	1.65
	XIV [b]	33.2	409	438	1615	62	70	10	15	5	1155	1539	1.33	1.12	1.10	0.92	924	1.67	–	–
[48]	OKJ-1	70.0	955	718	756	48	69	15	4	13	1148	1068	0.93	0.92	0.93	0.82	919	1.16	1.17	1.61
	OKJ-4	70.0	955	718	756	48	69	15	4	13	1148	1128	0.98	0.98	0.98	0.87	919	1.23	1.24	1.70
[49]	NO.2	34.1	354	354	180	46	64	27	0	9	655	485	0.74	1.10	1.04	1.13	524	0.92	0.86	1.05
	NO.4	34.1	354	354	180	46	71	19	0	10	594	542	0.91	1.22	1.16	1.26	476	1.14	0.96	1.17
[50]	J-1	81.2	638	638	834	48	72	14	2	12	1159	1150	0.99	1.08	1.00	1.04	927	1.24	1.04	1.49
	J-3	81.2	1456	1456	834	48	49	10	23	18	1694	1466	0.87	0.70	0.64	0.43	1355	1.08	1.32	1.90
	J-4	72.8	515	515	834	48	71	18	2	9	1143	1175	1.03	1.17	1.12	1.08	914	1.28	1.18	1.61
	J-5	72.8	839	839	834	48	69	14	3	15	1182	1320	1.12	1.13	1.09	0.95	946	1.40	1.33	1.81
	J-6	79.2	676	676	834	48	72	14	1	12	1152	1223	1.06	1.22	1.08	1.08	922	1.33	1.13	1.60
	J-8	79.2	370	370	834	48	66	20	1	13	1259	1385	1.10	1.31	1.18	1.04	1007	1.37	1.28	1.82
	J-10	39.2	700	700	417	48	61	19	3	17	873	875	1.00	0.98	1.08	0.78	698	1.25	1.47	1.63
	J-11	39.2	372	372	417	48	55	26	1	17	965	1029	1.07	1.20	1.26	0.81	772	1.33	1.72	1.92
[52]	JO-1	20.0	455	434	0	45	46	29	6	20	121	99	0.82	0.54	0.90	0.41	97	1.03	1.32	0.93

(continued on next page)

Table 2 (*continued*)

Author references	Specimen labels	f_c'(MPa)	f_{yh}(MPa)	f_{yv}(MPa)	N (kN)	θ_h(deg)	$V_{hc,ST1}$(%)	$V_{hc,ST2-3}$(%)	$V_{hs,h}$(%)	$V_{hs,v}$(%)	V_n(kN)	$V_{jh,test}$(kN)	$\frac{V_{jh,test}}{V_n}$	$\frac{V_{jh,test}}{V_{n,Kim}}$	$\frac{V_{jh,test}}{V_{n,Wang}}$	$\frac{V_{jh,test}}{V_{n,Kassem}}$	V_d(kN)	$\frac{V_{jh,test}}{V_d}$	$\frac{V_{jh,test}}{V_{d,EC8}}$	$\frac{V_{jh,test}}{V_{d,ACI}}$
[53]	J0C-1	31.2	447	343	88	48	80	16	3	0	140	159	1.14	1.05	1.37	1.24	112	1.42	1.62	1.33
[54]	1	41.3	320	473	511	51	58	24	12	6	1194	1001	0.84	0.85	0.89	0.84	955	1.05	1.10	1.36
[55]	1	34.0	305	476	996	55	67	22	8	4	1095	966	0.88	0.92	0.94	0.88	876	1.10	2.82	1.44
[56]	1 [a]	32.7	0	456	1557	63	85	15	0	0	946	985	1.04	-	-	-	757	1.30	-	-
	2 [a]	32.7	0	456	1557	63	85	15	0	0	946	969	1.02	-	-	-	757	1.28	-	-
	3 [a]	30.4	0	486	1557	64	84	16	0	0	905	936	1.03	-	-	-	724	1.29	-	-
	4 [b]	31.9	300	518	1557	63	80	15	1	4	982	923	0.94	1.09	0.91	0.68	786	1.17	-	-
	5 [b]	29.8	300	455	1557	64	80	15	2	4	948	954	1.01	0.95	0.95	0.64	758	1.26	-	-
[57]	S3	28.0	390	450	100	46	56	24	2	18	601	731	1.22	1.15	1.41	1.01	481	1.52	1.56	1.74
[58]	J3B	23.7	448	480	207	44	54	21	7	18	542	438	0.81	0.77	0.82	0.76	434	1.01	1.82	1.30
[59]	Ho-JI1 [a]	27.0	0	541	0	45	63	23	0	14	829	893	1.08	-	-	-	663	1.35	-	-
	Ko-JI1 [a]	32.0	0	533	403	62	60	29	0	11	554	759	1.37	-	-	-	443	1.71	-	-
[60]	BL1	28.8	407	528	1152	58	71	17	9	3	1083	1190	1.10	0.97	1.07	0.92	867	1.37	5.08	1.40
	BL2 [b]	37.5	368	540	1800	59	77	12	8	3	1322	1267	0.96	0.90	0.88	0.81	1058	1.20	-	-
	BL3	29.8	464	444	1173	48	76	15	7	3	1283	1034	0.81	0.81	0.81	0.86	1026	1.01	3.88	1.33
	BL4	32.8	362	553	1312	58	73	16	8	3	1178	1038	0.88	0.81	0.86	0.76	942	1.10	3.12	1.22

[a] Joints without horizontal hoops.
[b] Joints that did not satisfy both ACI Code and EC8 requirements.

$$V_n = q_1\left[4a_1\left(\frac{A_{sb1}}{\Phi_{b1}} + \frac{A_{sb2}}{\Phi_{b2}}\right)l_h + \chi f_c^{'} a_c b_j \cos\theta_h + a_2 A_{sh} f_{yh} + a_3\frac{A_{sv}f_{yv}}{\tan\theta_h}\right] \quad (37)$$

where $a_1 = q_0/q_1$, $a_2 = q_2/q_1$, and $a_3 = q_3/q_1$.

The coefficient q_1 is determined herein by imposing that the average (AVG) of the ratios between the experimental shear strength values and the nominal shear strength computed with Eq. (35), $V_{jh,test}/V_n$, is equal to 1.0. This constrain enforces the accuracy of the proposed expression for shear strength.

The coefficients, a_1, a_2, and $a_3$are determined by imposing that coefficient of variation (COV) of the ratios$V_{jh,test}/V_n$ is minimum. This constrain minimizes the scattering of the predicted results.

The values $q_0 = 1.32$, $q_1 = 0.80$, $q_2 = 0.14$ and $q_3 = 0.22$ have been determined accordingly, hence Eq. (35) becomes

$$V_n = 5.28\left(\frac{A_{sb1}}{\Phi_{b1}} + \frac{A_{sb2}}{\Phi_{b2}}\right)l_h + 0.80\chi f_c^{'} a_c b_j \cos\theta_h + 0.14 A_{sh} f_{yh} + 0.22\frac{A_{sv}f_{yv}}{\tan\theta_h} \quad (38)$$

For the 69 interior joints tested, Eq. (38) provides a COV value of 0.139. In Fig. 5 the ratios $V_{jh,test}/V_n$ versus $V_{jh,test}$ values for the 69 specimens are reported. It can be observed the low scattering of the predictions.

By using Eq. (38) it is also possible to plot the percentage of the contributions offered by the different resisting mechanisms related to the specific specimen, by sorting them in ascending order of the concrete struts' contribution to the total horizontal shear strength (Fig. 5).

On the basis of Fig. 6, with the support of Tables 1 and 2, the following observations can be made.

- The concrete struts' shear strength contribution is always greater than those offered by the joint horizontal stirrups and vertical intermediate reinforcement. The ST1 strut contribution is the greatest and ranges from 46% to 85% of the total shear strength. The contributions of ST2-3 struts is minor and ranges from 7% to 35%. It can be observed than an increase in the ST1 contribution involves a decrease in the ST2-3 contributions. The minimum percentage of shear force carried by the three strut mechanisms is equal to 59% and is achieved in specimen J-3 [50], which has a horizontal joint reinforcement ratio $\rho_h = \frac{A_{sh}}{h_b b_j}$ equal to 2.16%, just a little less than the maximum ρ_h, which is equal to 2.31%. The corresponding percentage of vertical joint reinforcement effective in resisting horizontal shear forces is $\rho_v = \frac{A_{sv}}{h_c b_j \tan\theta_h}$ equal to 1.07%, quite lower than the maximum ρ_v, which is equal to 2.66%.

For specimens J-MO and J-HO [32], with no vertical joint reinforcement and with identical yield strength of horizontal stirrups, it is observed that a doubling of horizontal joint reinforcement ratio ρ_h (from 0.65% to 1.29%) results in an equivalent increase in the shear strength percentage carried by the horizontal stirrups (from 5.4% to 10.2%).

For specimens J-OH [32] and E0.0 [28], with no horizontal joint reinforcement and with similar yield strength of joint vertical intermediate reinforcement, it is observed that an increase in ρ_v of about 68% (from 0.80% to 1.34%) entails a 50% increase in the shear strength contribution provided by vertical joint reinforcement (from 13% to 20%). The gap between the two increments is probably due to the difference in the yield strength of 11% from specimens J-OH to E0.0.

It can be concluded that, in the proposed model, the three strut mechanisms provide a predominant contribution in carrying the joint shear forces, even in the presence of appreciable amounts of vertical and horizontal joint reinforcements.

- The maximum shear strength percentage resisted by the horizontal stirrups is equal to 23% and it is attained in specimen J-3 [50], which has a horizontal joint reinforcement ratio ρ_h equal to 2.16%,

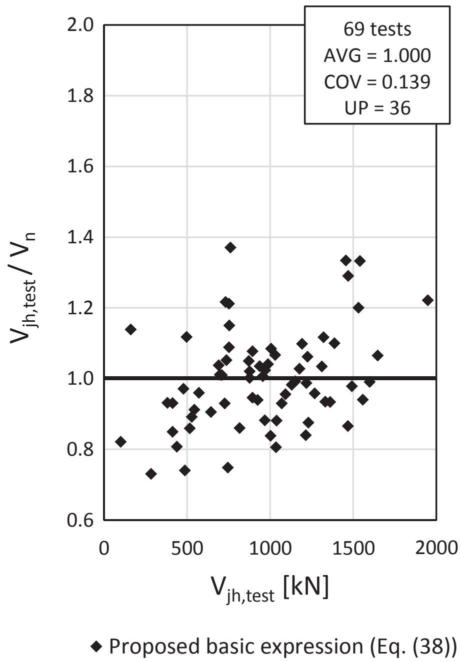

Fig. 5. $\mathbf{V_{jh,test}/V_n}$ ratios versus $\mathbf{V_{jh,test}}$ values.

and tensile strength of this reinforcement equal to 1456 MPa. Specimen 1 [54] having the maximum value of ρ_h, equal to 2.31%, provides instead a shear strength contribution of 12%. In this case, however, the tensile strength of joint horizontal stirrups is equal to 320 MPa. By comparing the two specimens and the results obtained for them, it can be observed that, even though the two specimens have nearly the same values of ρ_h and horizontal stirrups with yield strengths that differ more than 4.5 times from each other, the ratio between the shear strength percentages carried by these reinforcements is not equal to 4.5. This behavior can be understood by considering that the concrete strength of specimen J-3 [50] is twice that of specimen 1 [54]. Thus, as it can be seen from Eq. (38), the contribution of the strut mechanisms to joint shear strength is greater for the first specimen, in spite of the contribution carried by the horizontal stirrups.

Hence, the percentage of shear strength provided by the horizontal stirrups does not depend only on the horizontal joint reinforcement ratio ρ_h, but also on the tensile strength of this reinforcement and the percentage of shear strength that can be carried by strut mechanisms, which is strictly related to the concrete compression strength.

- Specimens with identical geometrical and mechanical properties but different axial load values in the column exhibit different horizontal shear strength. In particular, the greater the compression force N on the column, the greater is the joint horizontal shear strength. The increase in the compression force acting in the column induces an increase in θ_h, which leads to a decrease in the vertical joint reinforcement contribution to horizontal shear strength and a simultaneous increase in the concrete struts shear strength contribution. For specimens V [46] and VI [46] it is been observed that an increase in N of 1153% leads to an increase in θ_h of about 30%, which induces a simultaneous decrease in $\cos\theta_h$ and increase in a_c, causing an increase in concrete struts contribution of 42% and a decrease in the vertical joint reinforcement contribution of about 39%. Overall, the total shear strength increases thanks to the increase in the column compressive force.
- In specimens I [46] and III [46], having identical geometrical and mechanical properties and the same compression force acting in the column, but different amounts of vertical joint reinforcement, an increase of 290% in vertical joint reinforcement induces an increase of 13% in the shear strength and only an increase of 1% in the shear force carried by strut mechanisms. Hence it can be concluded that the increase of A_{sv} increases the shear strength, but does not entail a variation in the concrete compression stresses.

4. Existing models

To assess the reliability of the proposed formula, a comparison between the values of joint shear strength obtained from Eq. (38) and those obtained from models of Kim and LaFave [6], Wang et al. [7] and Kassem [8] is performed.

4.1. Kim and LaFave

In their research Kim and LaFave introduced an empirical model [6] to evaluate shear strength of joints with horizontal reinforcement, using the Bayesian parameter estimation method.

From the evaluation of an experimental database of RC beam-column connections, the authors proposed the following simplified formula for RC joint shear strength, which includes six key parameters

$$V_{jh} = 1.31\alpha_t\beta_t\eta_t(\mathrm{JI})^{0.15}(\mathrm{BI})^{0.30}(f_c^{'})^{0.75}A_{jh} \tag{39}$$

where α_t is a parameter for qualifying the in-plane geometry (1.0 for interior joints), β_t is a parameter for qualifying the out-of-plane geometry (1.0 for in-plane sub-assemblages), η_t describes joint eccentricity (1.0 for no eccentricity), JI is the joint transverse reinforcement index ($\mathrm{JI} = (\rho_j \bullet f_{yj})/f_c^{'}$) and BI the beam reinforcement index ($\mathrm{BI} = (\rho_b \bullet f_{yb})/f_c^{'}$).

4.2. Wang et al.

Wang et al. introduced a shear strength model [7], in which the reinforced concrete in the joint core is idealised as a homogeneous material in a plane stress state. The contribution of the joint shear reinforcement includes both the horizontal stirrups and the intermediate vertical bars of the column, and it is taken into account through the nominal tensile strength of the idealized concrete, $f_{t,n}$.

The critical shear force of the proposed model for interior beam-column joints is

$$V_{jh,max} = \frac{1 - (\sin^2\alpha/f_{t,n} - 0.8\cos^2\alpha/f_c^{'})\sigma_y}{(1/f_{t,n} + 0.8/f_c^{'})\sin 2\alpha}b_j h_c \tag{40}$$

where

$$f_{t,n} = f_{tc} + \rho_{sh}f_{yh}\cos^2\alpha + \rho_{sv}f_{yv}\sin^2\alpha \tag{41}$$

with

$$f_{tc} = 0.556\sqrt{f_c^{'}} \tag{42}$$

$$\alpha = \tan^{-1}(h_c/h_b) \tag{43}$$

$$\sigma_y = \frac{N}{b_c h_c} \tag{44}$$

4.3. Kassem

Kassem developed a mathematical method [8], built on the strut-and-tie model, to estimate the shear strength of reinforced concrete beam-column joints. The proposed model takes into account the shear stress contributions provided by the diagonal concrete strut and both horizontal stirrups and vertical intermediate column bars. The relevant explicit formula to evaluate the shear strength of interior joints is

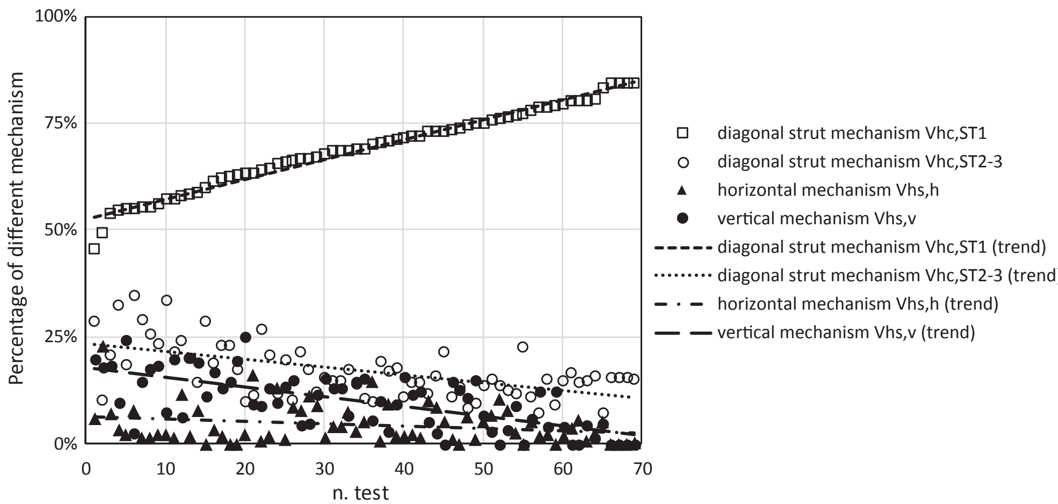

Fig. 6. Ratios of force distribution among the resisting mechanisms.

$$V_{jh} = \left(0.26[\psi\cos(\phi)] + 0.44\left[\omega_h + 1.39\omega_b\left(\frac{b_b}{b_j}\right)\tan(\phi)\right] + 0.07\left[\omega_v\left(\frac{b_c}{b_j}\right)\cot(\phi)\right]\right)f_c^{'}b_c h_c \tag{45}$$

where

$$\psi = 0.6\left(1 - \frac{f_c^{'}}{250}\right) \quad (f_c^{'} \text{ in MPa}) \tag{46}$$

$$\phi = \tan^{-1}(h_b/h_c) \tag{47}$$

$$\omega_h = (\rho_{jh} \cdot f_{yh})/f_c^{'} \tag{48}$$

$$\omega_b = (\rho_b \cdot f_{yb})/f_c^{'} \tag{49}$$

$$\omega_v = (\rho_c \cdot f_{yv})/f_c^{'} \tag{50}$$

4.4. Model reliability

The shear strength values, V_n, of 28 collected interior RC beam-column joints (data listed in Tables 3 and 4), different from those used for the coefficients' calibration, have been calculated applying the proposed formula (Eq. (38)), and the expressions of Kim and La Fave (Eq. (39)), Wang et al. (Eq. (40)) and Kassem (Eq. (45)). The authors decided to compare different models on a set of data (28 specimens) different from that used for the calibration of the coefficients of the proposed formula (69 specimens), to demonstrate that the predictions of this formula are good in general, not only on the data set used for the calibration. The data set of 28 specimens can be considered adequately diversified and representative (see Tables 3 and 4).

The computed values, V_n, are reported in Table 4 next to the experimental ones, $V_{jh,test}$. In the table there are reported also the ratios $V_{jh,test}/V_n$ and these ratios are plotted in Fig. 7, where the corresponding values of AVG, COV and UP (number of Unsafe Predictions) are specified.

For these 28 tests, performed on beam-column connections with horizontal stirrups, the AVG and COV of $V_{jh,test}/V_n$ ratios result respectively equal to 0.944 and 0.172, for the model of Kim and LaFave, 1.082 and 0.181, for the procedure of Wang et al., 1.001 and 0.172, for the expression of Kassem, and 0.990 and 0.162, for the proposed formula (Eq. (38)).

A comparison has been performed also on 60 + 28 = 88 specimens (Tables 1–4), considering also the specimens used for the calibration, apart 9 joints without horizontal reinforcement, for which it was not possible to use the model of Kim and La Fave. The ratios $V_{jh,test}/V_n$ are plotted in Fig. 8, where the corresponding values of AVG, COV and UP are specified.

AVG and COV of $V_{jh,test}/V_n$ ratios result respectively equal to: 0.991 and 0.177, for the model of Kim and LaFave, 1.036 and 0.184, for the procedure of Wang et al., 0.923 and 0.219, for the expression of Kassem, and 0.994 and 0.145, for the proposed formula (Eq. (38)).

Since both in comparison with 28 specimens and 88 ones the proposed shear strength formula provides the lowest COV value, it can be said it is more consistent than the other considered formulae. Moreover, it is adequately accurate, since it provides AVG values very close to 1.

4.5. Value of the proposed strategy

From the comparison with other models, it emerges how the proposed shear strength formula (Eq. (38)) provides accurate and consistent predictions for a wide range of specimens, representative of joints of both new and existing RC buildings, and also considering specimens completely independent from those used for its calibration (see results for the data set of 28 specimens in Fig. 7).

With respect to the formula provided by Kim and LaFave [6], given by Eq. (39), the proposed formula well predicts also shear strength of joints without horizontal reinforcement, while Eq. (39) is not usable in this case.

With respect to the formula of Wang et al. [7] (Eq. (40)), the advantage of the proposed formula is that it allows to separately calculate the contributions of the concrete struts and the truss mechanism, similarly to the formula proposed by Kassem [8] (Eq. (45)). However, differently from the last, the proposed formula takes into account also the influence of the column axial load.

The possibility to separately calculate the shear strength contributions enables to accurately evaluate, case by case, which, among these contributions, is the most prominent. This can be useful for further developments in the fields of buildings seismic assessment and retrofitting.

5. Design formula

The proposed shear strength formula (Eq. (38)) provides accurate and consistent predictions, as assessed through the comparison with other authors' formulae. However, since formula (38) presents an AVG equal to one, it is necessary to introduce a safety factor to employ it for

Table 3
Geometrical properties and reinforcement areas of the 28 specimens employed for the comparison between Eq. (38) and the expressions provided by Kim and LaFave (Eq. (39)), Wang et al. (Eq. (40)) and Kassem (Eq. (45)), and for the comparison between Eq. (51) and the shear strength formulae for interior joints provided by Eurocode 8 (Eq. (52)) and ACI 318–14 (Eq. (53)).

Author references	Specimen labels	b_b(mm)	h_b(mm)	b_c(mm)	h_c(mm)	δ_{b1}(mm)	δ_{b2}(mm)	δ_c(mm)	A_{sb1}(mm^2)	A_{sb2}(mm^2)	ϕ_1(mm)	ϕ_2(mm)	A_{sh}(mm^2)	A_{sv}(mm^2)
[27]	LIJ3	343	343	343	457	57	57	56	855	855	19.1	19.1	142	0
	LIJ4	343	343	343	457	54	54	56	633	633	12.7	12.7	142	0
[30]	X1	279	419	362	362	38	38	47	1551	1140	22.2	19.1	865	1013
	X2	279	419	362	362	38	38	47	1551	1140	22.2	19.1	1297	1013
	X3	279	419	362	362	38	38	47	1163	855	22.2	19.1	865	570
[34]	S1	350	500	500	460	53	53	55	2026	1013	25.4	25.4	1592	2026
[35]	C1-400	350	500	500	550	58	51	68	3020	1520	23.3	22.0	2123	2641
	C2-600	350	500	500	550	51	51	68	1900	1140	22.0	22.0	2123	2641
	C3-600	350	500	500	450	51	51	68	1900	1140	22.0	22.0	2123	2641
	C4-600	350	500	500	550	53	53	68	1963	981	25.0	25.0	2123	2641
[36]	PL-13	200	350	300	300	32	32	32	663	663	13.0	13.0	339	402
	PH-16	200	350	300	300	32	32	32	804	804	16.0	16.0	452	402
	PH-13	200	350	300	300	57	57	32	929	929	13.0	13.0	452	402
	PH-10	200	350	300	300	48	48	32	785	785	10.0	10.0	452	402
[43]	J1	300	400	350	350	57	57	55	2010	2010	16.0	16.0	942	2641
	BJ1	300	400	350	350	48	48	55	1206	1206	16.0	16.0	942	2641
	BJ2	300	400	350	350	48	48	55	1005	1005	16.0	16.0	628	2641
	BJ3	300	400	350	350	48	48	55	804	804	16.0	16.0	628	2641
[44]	BCJ2	203	305	254	254	27	25	27	506	285	12.7	9.5	127	760
	BCJ3	203	305	254	304	27	25	27	506	285	12.7	9.5	127	760
[47]	No. 1 [b]	250	350	350	350	38	38	34	1963	1963	25.0	25.0	471	2280
	No. 5 [b]	250	350	350	350	51	51	34	1407	1407	16.0	16.0	471	2280
[51]	C1	200	300	300	300	45	30	30	855	427	9.5	9.5	191	760
	J3	200	300	300	300	45	30	30	1013	507	12.7	12.7	899	760
[60]	CL1	350	500	400	400	38	38	38	1407	1206	16.0	16.0	1809	402
	CL2 [b]	300	500	400	400	52	40	40	1884	1256	20.0	20.0	2035	628
	CL3	250	400	350	450	54	36	36	1608	804	16.0	16.0	1356	402
	CL4	300	500	400	400	47	38	38	1608	1005	16.0	16.0	2035	402

[b] Joints that did not satisfy both ACI Code and EC8 requirements.

design purposes.

It is possible to provide a design shear strength formula by multiplying Eq. (38) by a safety factor, without altering the COV value. The safety factor is determined on statistical basis here, so that there is a 95% probability that the predicted design shear strength is lower than the experimental one for the 69 test data used for the coefficients' calibration.

The proposed design formula derived is

$$V_{\mathrm{n,d}} = 0.80\left[5.28\left(\frac{A_{\mathrm{sb1}}}{\Phi_{\mathrm{b1}}} + \frac{A_{\mathrm{sb2}}}{\Phi_{\mathrm{b2}}}\right)l_{\mathrm{h}} + 0.80\chi f_{\mathrm{c}}^{'} a_{\mathrm{c}} b_{\mathrm{j}} \cos\theta_{\mathrm{h}} + 0.14 A_{\mathrm{sh}} f_{\mathrm{yh}} + 0.22\frac{A_{\mathrm{sv}} f_{\mathrm{yv}}}{\tan\theta_{\mathrm{h}}}\right] \tag{51}$$

which provides AVG = 1.250.

To assess the reliability of this formula, a comparison with the formulae for interior joints provided by Eurocode 8 [1] and ACI 318–14 [2] is performed on 25 specimens, using the test data employed for the comparison with the existing models, apart 3 joints which do not satisfy both Codes requirements (Tables 3-4).

5.1. *Eurocode 8* [1]

In Eurocode 8 [1] the maximum horizontal shear force allowed in interior beam-column joints is

$$V_{\mathrm{jhd}} = \eta f_{\mathrm{cd}} b_{\mathrm{j}} h_{\mathrm{jc}} \sqrt{1 - \frac{\nu_{\mathrm{d}}}{\eta}} \tag{52}$$

where $\eta = 0.6\left(1 - \frac{f_{\mathrm{c}}^{'}}{250}\right)$, ν_{d} is the normalised axial force in the column above the joint and h_{jc} is the distance between the extreme layers of column reinforcement.

5.2. *ACI Code 318–14* [2]

The nominal shear strength of interior beam-column joints in ACI Code 318–14 [2] is calculated accounting the compressive strength of the concrete and the geometry of the joint, through the following design formula

$$V_{\mathrm{d}} = \phi V_{\mathrm{n}} = \phi \cdot 0.083\gamma\sqrt{f_{\mathrm{c}}^{'}}\, b_{\mathrm{j}} h_{\mathrm{c}} \tag{53}$$

where $\phi = 0.85$, γ is equal to 15 for joints confined by beams on two opposite faces, with beam widths at least three-quarters of the effective joint width, and $\gamma = 12$ for beam widths smaller than three-quarters of the effective joint width. The effective joint width b_{j} should not exceed the smallest of $(b_{\mathrm{b}} + b_{\mathrm{c}})/2$, $b + 2x$ where x is the smaller distance from the beam vertical edges to the closest column vertical edges [2].

5.3. *Comparison*

All the 25 collected tests satisfy both ACI Code and Eurocode 8 requirements for beam-column connections and are considered in the comparison with both Codes (Fig. 9). In Eq. (38) the average value of concrete strength is used, i.e. $f'_c = f_{cm}$, while in Eq. (52), the design value, i.e. $f_{cd} = (f_{cm} - 8)/1.5$, and in Eq. (53), the specified one, i.e. $f'_c = f_{cm} - 8$, are used.

The computed shear strength values, V_{d}, are reported in Table 4 next to the experimental ones, $V_{\mathrm{jh,test}}$. In the table there are reported also the ratios $V_{\mathrm{jh,test}}/V_{\mathrm{d}}$ and these ratios are plotted in Fig. 9

The ratios between the experimental results relevant the 25 collected interior joints and the results obtained by the application of the proposed design shear strength formula (Eq. (51)) give an AVG equal to 1.216 and a COV of 0.149. The Unsafe Predictions (UP) are 2.

For Eurocode 8 and ACI Code 318–148, the AVG and COV values of the $V_{\mathrm{jh,test}}/V_{\mathrm{d}}$ ratios and UP are respectively equal to 1.420, 0.501 and 7, and 1.439 0.216 and 2.

Table 4
Mechanical properties, forces and results of the 28 specimens employed for the comparison between Eq. (38) and the expressions provided by Kim and LaFave (Eq. (39)), Wang et al. (Eq. (40)) and Kassem (Eq. (45)), and for the comparison between Eq. (51) and the shear strength formulae for interior joints provided by Eurocode 8 (Eq. (52)) and ACI 318–14 (Eq. (53)).

Author references	Specimen labels	f_c' (MPa)	f_{yh} (MPa)	f_{yv} (MPa)	N (kN)	θ_h (deg)	$V_{hc,ST1}$ (%)	$V_{hc,ST2-3}$ (%)	$V_{hs,h}$ (%)	$V_{hs,v}$ (%)	V_n (kN)	$V_{jh,test}$ (kN)	V_d (kN)	$\frac{V_{jh,test}}{V_n}$	$\frac{V_{jh,test}}{V_{n,Kim}}$	$\frac{V_{jh,test}}{V_{n,Wang}}$	$\frac{V_{jh,test}}{V_{n,Kassem}}$	$\frac{V_{jh,test}}{V_d}$	$\frac{V_{jh,test}}{V_{d,EC8}}$	$\frac{V_{jh,test}}{V_{d,ACI}}$
[27]	LIJ3	31.1	400	470	0	37	79	20	1	0	824	724	659	0.88	0.79	1.47	1.10	1.10	0.73	0.91
	LIJ4	34.3	400	470	0	37	79	20	1	0	900	789	720	0.88	0.91	1.52	1.46	1.10	0.71	0.93
[30]	X1	34.3	352	414	225	50	65	21	5	9	847	840	678	0.99	0.92	1.13	1.05	1.24	1.02	1.33
	X2	33.6	352	414	264	51	64	20	7	9	868	853	695	0.98	0.88	1.06	0.99	1.23	1.08	1.37
	X3	31.0	352	414	203	50	70	18	6	6	724	629	579	0.87	0.77	0.96	0.98	1.09	0.86	1.07
[34]	S1	38.3	496	452	0	47	66	15	7	12	1478	1419	1183	0.96	0.82	1.01	1.00	1.20	0.76	1.25
[35]	C1-400	32.0	446	510	0	42	55	22	7	16	1973	1860	1579	0.94	0.81	1.06	0.88	1.18	1.03	1.53
	C2-600	32.0	446	510	0	42	59	16	7	18	1841	1842	1473	1.00	0.80	1.05	0.88	1.25	1.02	1.52
	C3-600	32.0	446	510	0	48	56	17	9	18	1444	1853	1156	1.28	0.98	1.24	0.95	1.60	1.36	1.87
	C4-600	29.6	446	510	0	42	59	15	7	19	1724	1832	1379	1.06	0.85	1.07	0.96	1.33	1.12	1.59
[36]	PL-13	26.4	366	402	396	54	73	19	3	5	517	449	414	0.87	0.91	0.96	1.03	1.08	1.56	1.32
	PH-16	23.6	366	402	354	54	70	20	5	5	484	482	387	0.99	0.93	1.06	0.99	1.24	2.03	1.54
	PH-13	26.3	366	402	395	54	67	25	4	5	561	544	449	0.97	0.96	1.13	0.96	1.21	1.90	1.60
	PH-10	25.6	366	402	384	54	65	27	4	5	565	512	452	0.91	0.95	1.08	1.00	1.13	1.87	1.54
[43]	J1	40.0	510	514	0	49	44	29	5	22	1193	1604	955	1.34	1.25	1.52	0.99	1.68	1.70	2.36
	BJ1	40.0	510	514	0	49	49	20	6	25	1054	1237	843	1.17	1.12	1.17	1.10	1.47	1.31	1.82
	BJ2	40.0	510	514	0	49	52	17	4	26	997	1061	798	1.06	1.08	1.06	1.13	1.33	1.13	1.56
	BJ3	40.0	510	514	0	49	54	15	5	27	962	920	770	0.96	1.00	0.92	1.13	1.20	0.98	1.35
[44]	BCJ2	30.3	414	448	0	50	60	20	2	18	350	358	280	1.02	1.07	1.11	1.27	1.28	0.86	1.23
	BCJ3	27.4	414	448	0	45	61	20	2	18	419	394	335	0.94	1.01	1.09	1.32	1.17	0.86	1.22
[47]	No. 1 [b]	22.1	377	548	833	54	61	15	3	22	935	1148	–	1.23	1.19	1.13	0.75	–	–	–
	No. 5 [b]	21.6	377	548	833	54	59	17	3	21	940	1244	–	1.32	1.44	1.24	1.06	–	–	–
[51]	C1	26.6	324	422	183	47	61	26	1	11	571	436	457	0.76	0.95	0.95	1.13	0.95	1.05	1.27
	J3	24.0	367	374	173	47	58	23	8	10	554	576	443	1.04	0.88	1.12	0.90	1.30	1.62	1.81
[60]	CL1	35.5	407	528	1420	58	75	15	8	2	1237	1120	989	0.91	0.86	0.88	0.84	1.13	2.89	1.35
	CL2 [b]	38.2	368	540	1834	59	77	12	8	3	1337	1162	–	0.87	0.83	0.80	0.74	–	–	–
	CL3	34.3	464	444	1351	48	78	14	6	2	1409	945	1127	0.67	0.71	0.67	0.77	0.84	2.54	1.29
	CL4	30.2	362	553	1208	58	72	17	9	3	1118	947	894	0.85	0.76	0.83	0.70	1.06	3.49	1.36
													AVG	0.990	0.944	1.082	1.001	1.216	1.420	1.439
													DEV.ST	0.160	0.163	0.196	0.173	0.181	0.711	0.311
													COV	0.162	0.172	0.181	0.172	0.149	0.501	0.216
													UP	18	20	8	15	2	7	2

[b] Joints that did not satisfy both ACI Code and EC8 requirements.

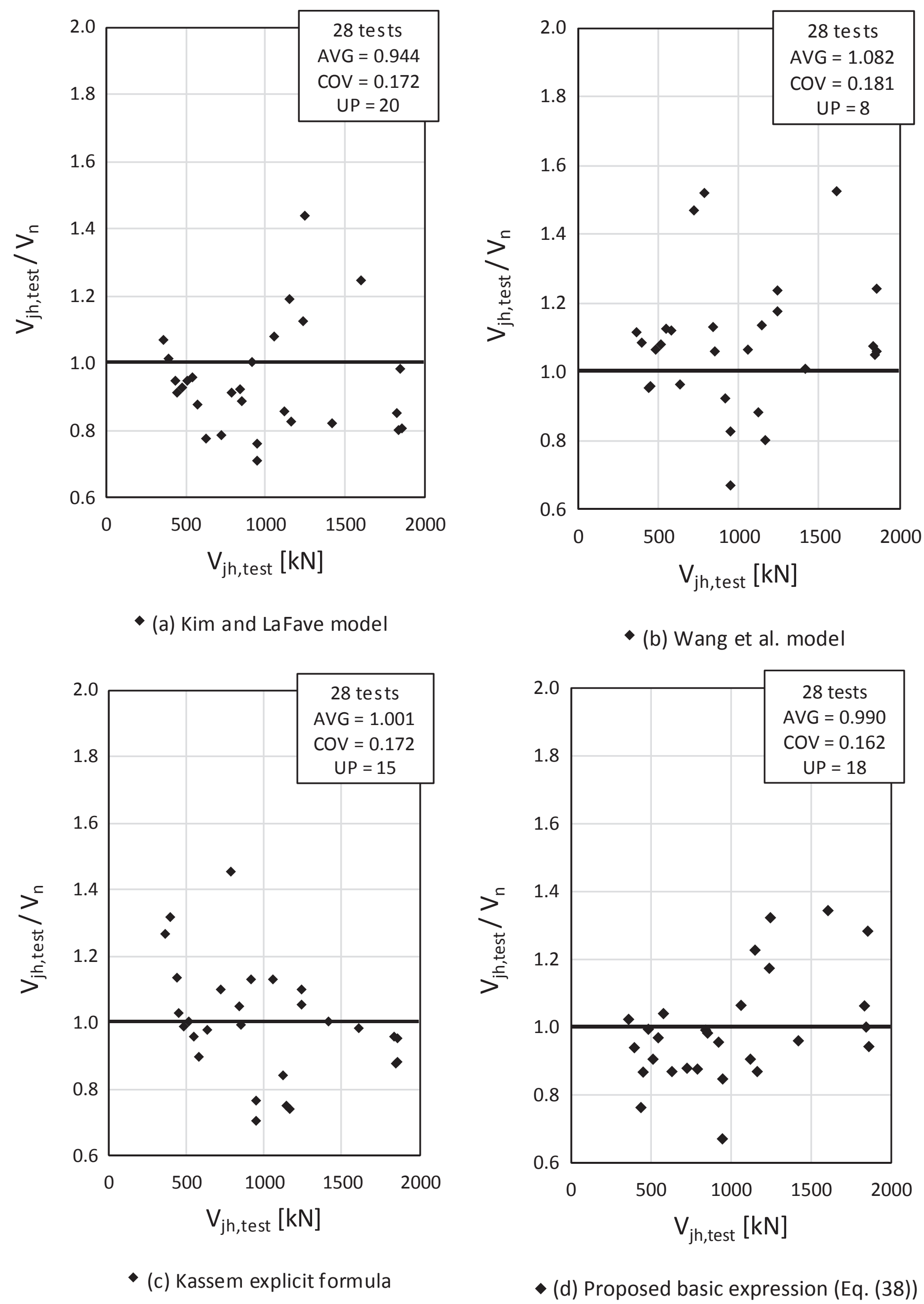

Fig. 7. Ratios $\mathbf{V_{jh,test}/V_n}$ versus $\mathbf{V_{jh,test}}$ values for 28 specimens calculated by means of (a) Kim and LaFave model, (b) Wang et al. model, (c) Kassem explicit formula and (d) proposed basic expression (Eq. (38)).

From this comparison, it is apparent that the proposed design formula (Eq. (51)) gives appropriately safe predictions, since it leads only to 2 UP, without being excessively conservative (lowest AVG value in comparison to ACI Code and Eurocode 8). Furthermore, the proposed formula is the most consistent, since it provides the lowest COV.

A comparison has been made also on a set of 40 + 25 = 65 specimens, considering also the specimens used for the calibration (Tables 1–4), apart 9 joints without horizontal reinforcement and 20 joints that did not satisfy both Codes requirements. The ratios $V_{jh,test}/V_d$ are plotted in Fig. 10, where the corresponding values of AVG, COV and UP are specified.

The AVG and COV of $V_{jh,test}/V_n$ ratios and UP result respectively equal to: 1.710, 0.663 and 14 for Eurocode 8, 1.370, 0.200 and 4 for ACI Code and 1.208, 0.134 and 5 for the proposed design formula. These results confirm the considerations previously made for the comparison with the data set of 25 specimens.

It can be observed that the COV values gained by the formulae of the Codes are much larger than those obtained by the proposed design formula, because the Code formulations are simplified and contain less parameters than the proposed one. The latter, on the contrary, takes account of a greater number of mechanical phenomena and this makes the prediction more consistent.

As regards the unsafe predictions, it is clear that the proposed formula and ACI Code provide results safer than Eurocode 8.

6. Conclusions

On the basis of a mechanical analysis and the use of 69 previous experimental results, a new model for the shear strength prediction of interior RC beam-column joints under seismic loads has been obtained,

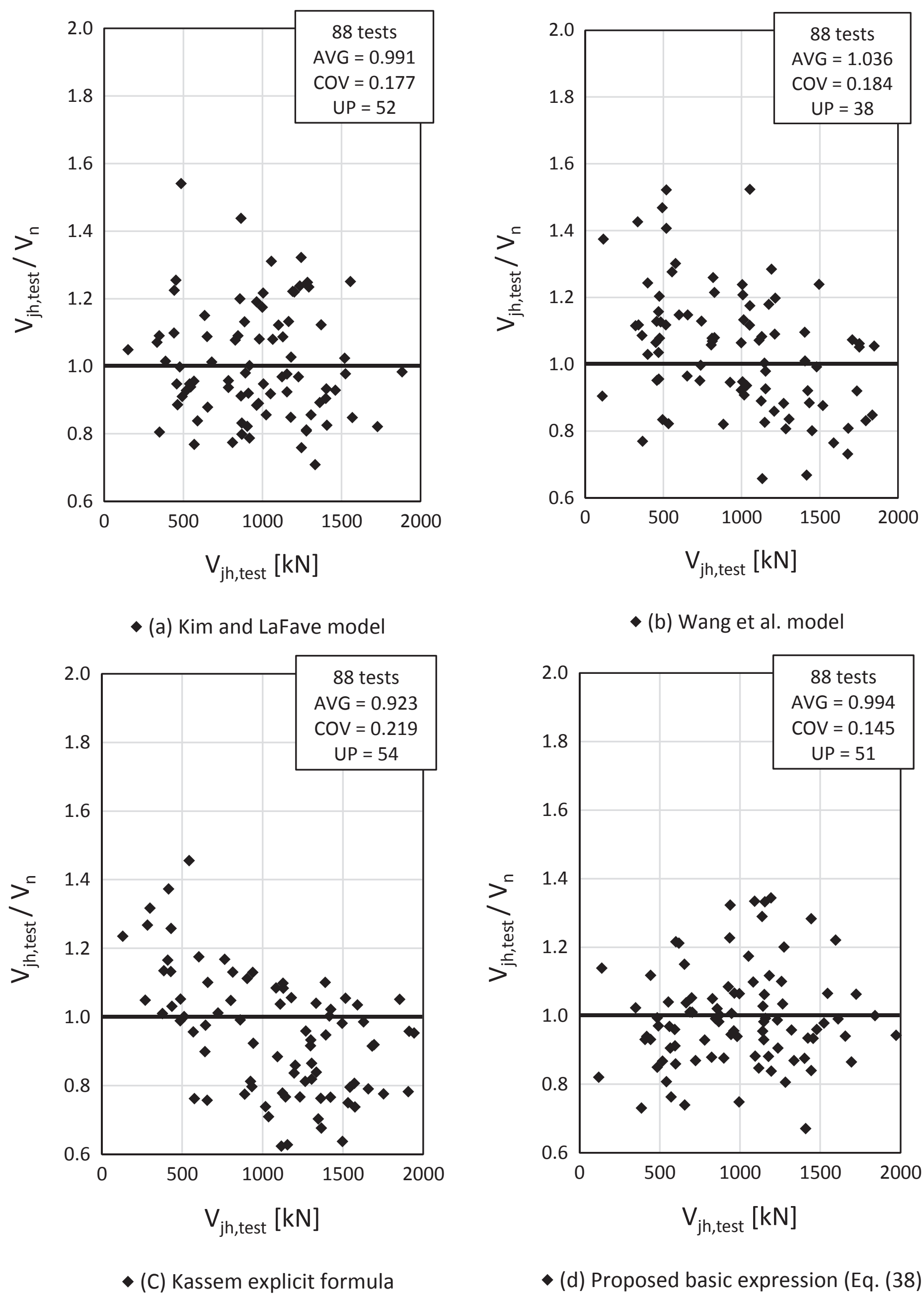

Fig. 8. Ratios $V_{jh,test}/V_n$ versus $V_{jh,test}$ values for 88 specimens calculated by means of (a) Kim and LaFave model, (b) Wang et al. model, (c) Kassem explicit formula and (d) proposed basic expression (Eq. (38)).

and the following conclusions can be drawn:

(1) The shear strength arises from the contribution of three inclined concrete struts and the contribution of horizontal stirrups and vertical reinforcement of the joint core. The model takes into account the column axial load influence on the inclination of the concrete struts.
(2) The sum of the three inclined concrete struts contributions constitute the main resisting mechanism.
(3) The percentage of shear strength provided by the horizontal stirrups depends not only on the horizontal joint reinforcement ratio ρ_h, but also on the tensile strength of the stirrups and the percentage of shear strength that can be carried by the strut mechanisms, which is strictly related to the concrete compression strength.
(4) An increase in the column axial compression load entails an increase in θ_h, which leads to a decrease in the vertical joint reinforcement contribution to horizontal shear strength and a simultaneous increase in the concrete strut shear strength contribution.
(5) In interior RC beam-column joints, vertical bars are more effective than horizontal stirrups in providing shear strength.
(6) In the experimental comparison with the formulae of Kim and LaFave, Wang et al. and Kassem, the proposed formula (Eq. (38)) gives the most consistent predictions, because it provides the the lowest COV value. Moreover, it is adequately accurate, since it provides AVG values very close to 1. Hence, it is possible to state that the proposed mechanical model well implements the actual mechanical behavior.
(7) A design formula (Eq. (51)) is derived on the basis of a conservative criterion, by multiplying Eq. (38) by a safety factor. The

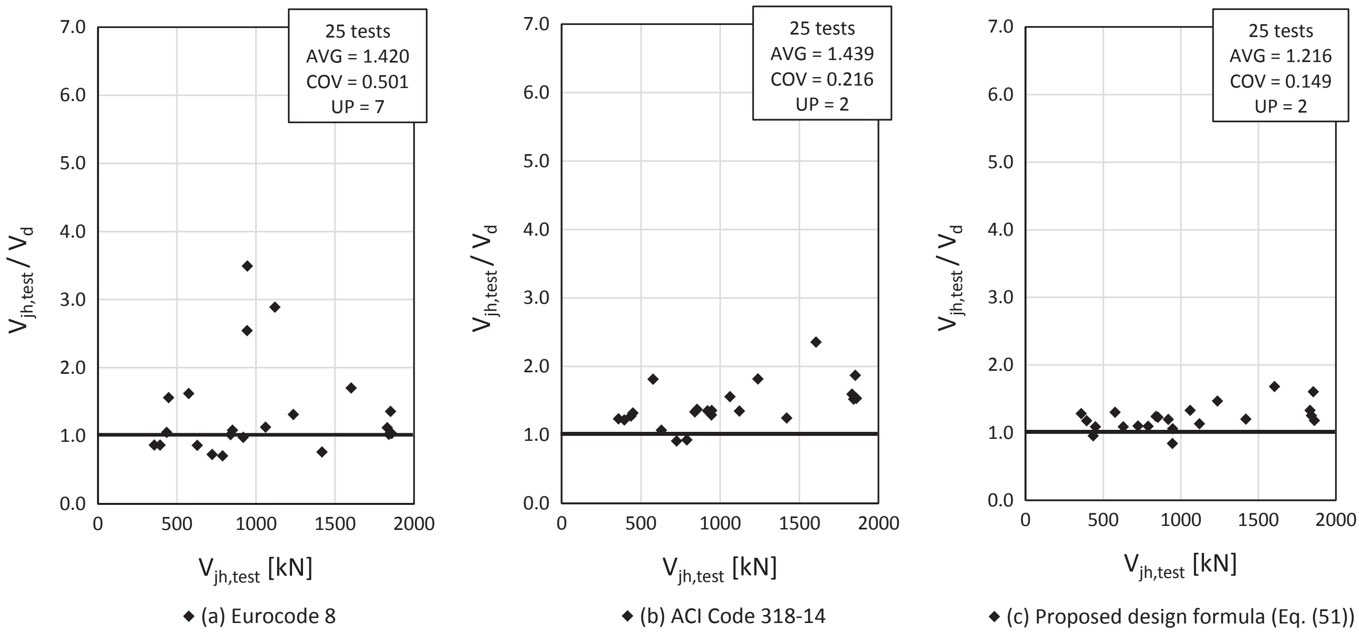

Fig. 9. Ratios $\mathbf{V_{jh,test}/V_d}$ versus $\mathbf{V_{jh,test}}$ values for 25 specimens calculated by means of (a) Eurocode 8, (b) ACI Code 318–14 and (c) proposed design formula (Eq. (51)).

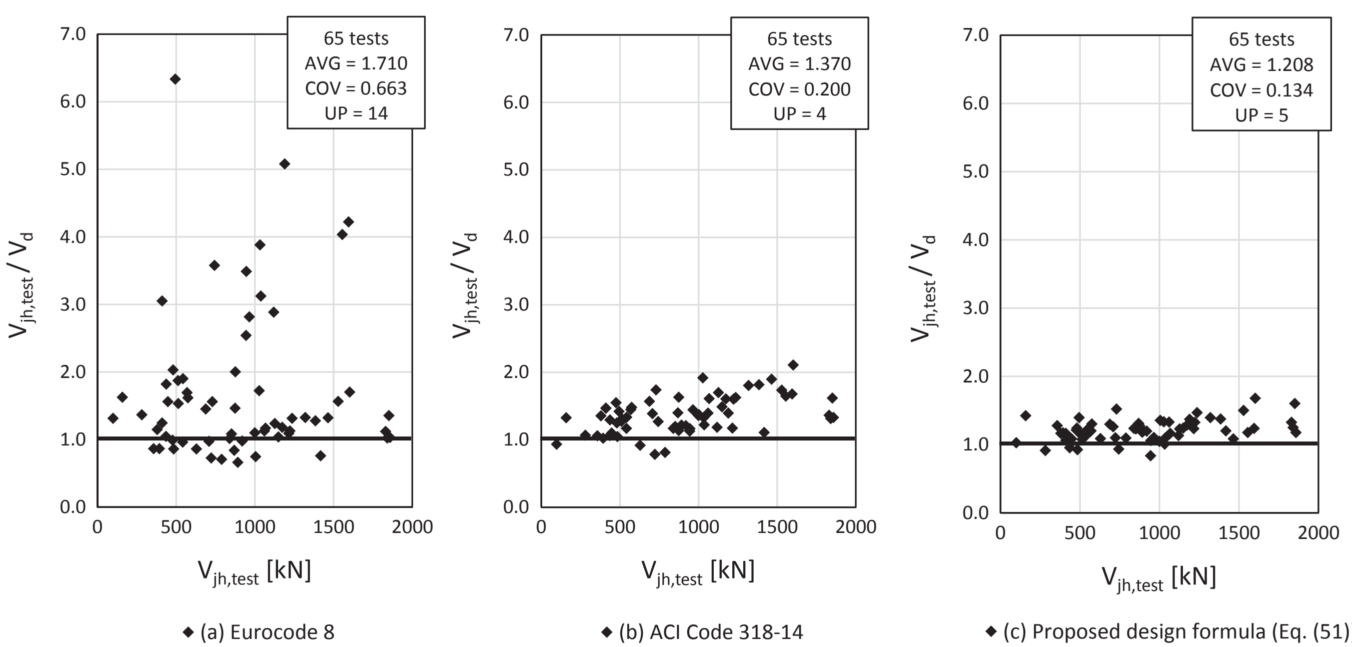

Fig. 10. Ratios $V_{jh,test}/V_d$ versus $V_{jh,test}$ values for 65 specimens calculated by means of (a) Eurocode 8, (b) ACI Code 318–14 and (c) proposed design formula (Eq. (51)).

experimental comparison, on a collection of 25 specimens, with the shear strength design formulae of Eurocode 8 and ACI Code 318–14 proves that the proposed design formula gives appropriately safe predictions, since it provides the lowest number of unsafe predictions, like ACI Code, without being excessively conservative, since it provides AVG values very close to 1. Furthermore, the proposed formula is the most consistent, since it provides the lowest COV value.

Declaration of Competing Interest

None.

Acknowledgements

The research has been funded by Italian Department of Civil Protection (Executive Projects DPC_ReLUIS 2014–2018).

Appendix A. Supplementary material

Supplementary data to this article can be found online at https://doi.org/10.1016/j.engstruct.2020.111223.

References

[1] Eurocode 8, UNI EN 1998-1:2005, Design of structures for earthquake resistance - Part 1: General rules, seismic actions and rules for buildings. CEN, Comité European de Normalisation; 2004.

[2] ACI Committee 318. Building code requirements for structural concrete (ACI 318-14) and commentary (ACI 318R-14). Farmington Hills; American Concrete Institute; 2014.

[3] Somma G, Pieretto A, Rossetto T, Grant DNRC. beam to column connection failure assessment and limit state design. Mater Struct 2015;48(4):1215–31.

[4] Somma G. Shear strength of beam-column joints under seismic loading-Fiber effectiveness. In: 3rd International fib Congress and Exhibition, Incorporating the PCI Annual Convention and Bridge Conference 2010, United States 2010; Code 126173.

[5] Russo G, Pauletta M. Seismic Behavior of Exterior Beam-Column Connections with Plain Bars and Effects of Upgrade. ACI Struct J 2012;109(2):225–33.

[6] Kim J, LaFave J. A simplified approach to joint shear behavior prediction of RC beam-column connections. Earthquake Spectra 2012;28(3):1071–96.

[7] Wang GL, Dai JG, Teng JG. Shear strength model for RC beam-column joints under seismic loading. Eng Struct 2012;40:350–60.

[8] Kassem W. Strut-and-tie modelling for the analysis and design of RC beam-column joints. Mater Struct 2016;49:3459–76.

[9] Unal M, Burak B. Joint shear strength prediction for reinforced concrete beam-to-column connections. Struct Eng Mech 2012;41(3):421–40.

[10] Russo G, Somma G, Angeli P, Mitri D. Contributi resistenti a taglio nei nodi interni soggetti ad azione sismica. In: XI National Congress "Seismic engineering in Italy". Genova, Italy; 2004. p. 25–9.

[11] Muhsen BA, Umemura H. New model for estimation of shear strength of reinforced concrete beam column joints. Proc Eng 2011;14:2151–9.

[12] Attaalla SA. General analytical model for nominal shear stress of type 2 normal- and high-strength concrete beam-column joints. ACI Struct J 2004;10(1):65–75.

[13] Hwang SJ, Lee HJ. Analytical model for predicting shear strengths of interior reinforced concrete beam–column joints for seismic resistance. ACI Struct J 2000;97(1):35–44.

[14] Massone LM, Orrego GN. Analytical model for shear strength estimation of reinforced concrete beam-column joints. Eng Struct 2018;173:681–92.

[15] Pan Z, Guner S, Vecchio FJ. Modeling of interior beam-column joints for nonlinear analysis of reinforced concrete frames. Eng Struct 2017;142:182–91.

[16] Wong HF, Kuang JS. Predicting shear strength of RC interior beam-column joints by modified rotating-angle softened-truss model. Comput Struct 2014;133:12–7.

[17] Park S, Mosalam KM. Analytical model for predicting shear strength of unreinforced exterior beam-column joints. ACI Struct J 2012;109(2):149–59.

[18] Pauletta M, Di Luca D, Russo G. Exterior beam-column joints – Shear strength model and design formula. Eng Struct 2015;94:70–81.

[19] Hwang SJ, Lee HJ. Analytical model for predicting shear strengths of exterior reinforced concrete beam–column joints for seismic resistance. ACI Struct J 1999;96(5):846–57.

[21] Paulay T, Priestley MJN. Seismic design of reinforced concrete and masonry buildings. New York: John Wiley and Sons; 1992.

[22] Russo G, Venir R, Pauletta M, Somma G. Reinforced concrete corbels – shear strength model and design formula. ACI Struct J 2006;103(1):3–10.

[23] Russo G, Venir R, Pauletta M. Reinforced concrete deep beams – shear strength model and design formula. ACI Struct J 2005;102(3):429–37.

[24] Russo G, Pauletta M. A simple method for evaluating the maximum slip of anchorages. Mater Struct 2006;39:533–46. https://doi.org/10.1617/s11527-006-9092-1.

[25] Russo G, Pauletta M, Mitri D. Solution for bond distribution in asymmetric R.C. structural members. Eng Struct 2009;31(3):633–41.

[26] Piccinin R, Cattaneo S, Biolzi L. Breakout capacity of headed anchors in confined concrete: Experimental evidence. ACI Struct J 2013;110(3):469–79.

[27] Abrams DP. Scale relations for reinforced concrete beam-column joints. ACI Struct J 1987;84(6):502–12.

[28] Au FTK, Huang K, Pam HJ. Diagonally-reinforced beam-column joints reinforced under cyclic loading. Proc Inst Civil Eng: Struct Build 2005;158(1):21–40.

[29] Birss GR. The elastic behaviour of earthquake resistant reinforced concrete beam-column joints. Research Report No. 78-13. Department of Civil Engineering, University of Canterbury, Christchurch, New Zealand; 1978.

[30] Durrani AJ, Wight JK. Behavior of interior beam-to-column connections under earthquake-type loading. ACI J 1985;82(3):343–9.

[31] Fujii S, Morita S. Comparison between interior and exterior RC beam-column joint behavior. In: Jirsa JO, editor. Design of beam-column joints for seismic resistance, SP-123, American Concrete Institute, Farmington Hills, Mich. 1991; 145-165.

[32] Goto Y, Joh O. An experimental study of shear failure mechanism of RC interior beam-column joints. In: 11th World Conference on Earthquake Engineering, Acapulco Mexico; 1996; 1194.

[33] Hakuto S, Park R, Tanaka H. Seismic load tests on interior and exterior beam-column joints with substandard reinforcing details. ACI Struct J 2000;97(1):11–25.

[34] Hwang HJ, Eom TS, Park HG. Design considerations for interior RC beam-column joint with additional bars. Eng Struct 2015;98:1–13.

[35] Hwang HJ, Park HG, Choi WS, Chung L, Kim JK. Cyclic Loading Test for Beam-Column Connections with 600 MPa (87 ksi) Beam Flexural Reinforcing Bars. ACI Struct J 2014;111(4):913–24.

[36] Joh O, Goto Y. Beam-column joint behavior after beam yielding in r/c ductile frames. In: Proceedings of the 12th world conference on earthquake engineering. Auckland, New Zealand; 2000.

[37] Joh O, Goto Y, Shibata T. Behavior of Reinforced Concrete Beam-Column Joints with Eccentricity. In: Design of beam-column joints for seismic resistance, SP-123, American Concrete Institute, Detroit (MI); 1991. p. 317–57.

[38] Kamimura T, Takeda S, Tochio AM. Influence of joint reinforcement on strength and deformation of interior beam-column subassemblages. In: Proceedings of the 12th world conference on earthquake engineering. Auckland, New Zealand; 2000.

[39] Kitayama K, Lee S, Otani S, Aoyama H. Behavior of high-strength R/C beam-–column joints. In: Proceedings of the 10th world conference on earthquake engineering. Rotterdam, Holland; 1992. p. 3151–6.

[40] Kitayama K, Otani S, Aoyama H. Development of design criteria for RC interior beam column joints. Design of beam-column joints for seismic resistance, SP-123, American Concrete Institute, Farmington Hills, Mich; 1991. p. 97–123.

[41] Kusuhara F, Azukawa K, Shiohara H, Otani S. Tests of reinforced concrete interior beam-column joint subassemblage with eccentric beams. In: Proceedings of the 13th world conference on earthquake engineering. Vancouver, Canada; 2004.

[42] Lee WT, Chiou YJ, Shih MH. Reinforced concrete beam–column joint strengthened with carbon fiber reinforced polymer. Compos Struct 2010;92:48–60.

[43] Lee JY, Kim JY, Oh GJ. Strength deterioration of reinforced concrete beam-column joints subjected to cyclic loading. Eng Struct 2009;31:2070–85.

[44] Leon RT. Shear strength and hysteretic behavior of interior beam-column joints. ACI Struct J 1990;87(1):3–11.

[45] Li B, Tran C. Seismic behavior of reinforced concrete beam-column joints with vertically distributed reinforcement. ACI Struct J 2009;106(6):790–9.

[46] Meinheit DF, Jirsa JO. The shear strength of reinforced concrete beam-column joints. CESRL Report No. 77-1, University of Texas at Austin; 1977.

[47] Morita S, Kitayama K, Koyama A, Hosono T. Effects of beam bar bond and column axial load on shear strength in reinforced concrete interior beam-column joints. Trans Japan Concr Inst 1999;21:453–60.

[48] Noguchi H, Kashiwazaki T. Experimental studies on shear performances of RC interior beam-column joints with high-strength materials. In: Proceedings of the 10th world conference on earthquake engineering. Rotterdam, Holland; 1992. p. 3163–8.

[49] Noguchi H, Kurusu K. Correlation of bond and shear in RC beam-column connections subjected to seismic forces. In: Proceedings of the 9th world conference on earthquake engineering. Tokyo-Kyoto, Japan; 1988. p. 597–602.

[50] Oka K, Shiohara H. Tests of high strength concrete interior beam-column-joint subassemblages. In: Proceedings of the 10th world conference on earthquake engineering. Rotterdam; 1992. p. 3211–7.

[51] Otani S, Kitayama K, Aoyama H. Beam bar bond requirements for interior beam-column connections. In: Proceedings, International Symposium on Fundamental Theory of Reinforced Concrete and Prestressed Concrete, Nanjing Institute of Technology, China; 1986.

[52] Owada Y. Three dimensional behaviors of reinforced concrete beam–column joint under seismic load. In: Proceedings of the 12th world conference on earthquake engineering. Aukland, New Zealand; 2000.

[53] Owada Y. Seismic behavior of beam-column joint of reinforced concrete exterior frame under varying axial load. In: Proceedings of the 10th world conference on earthquake engineering. Rotterdam, Holland; 1992. p. 3181–4.

[54] Park R, Milburn JR. Comparison of recent New Zealand and United States seismic design provisions for reinforced concrete beam-column joints and tests results from four units designed according to the New Zealand code. Bull New Zealand Nat Soc Earthq Eng 1983;16(1):3–24.

[55] Park R, Gaerty L, Stevenson EC. Tests on an interior reinforced concrete beam-column joint. Bull New Zealand Nat Soc Earthq Eng 1981;14(2):81–92.

[56] Pessiki SP, Conley CH, Gergely P, White RN. Seismic behavior of lightly-reinforced concrete column and beam-column joint details: Report No. NCEER-90-0014. State University of New York, Buffalo; 1990.

[57] Shiohara H, Zaid S, Otani S. Test of innovative reinforcing detail for R/C interior beam-column connections subjected to seismic action. In: Proceedings of the Third International Conference on Concrete under Severe Conditions, University of British Columbia, Vancouver, Canada; 2001. p. 1:739–746.

[58] Supaviriyakit T, Pimanmas A. Comparative performance of sub-standard interior reinforced concrete beam–column connection with various joint reinforcing details. Mater Struct 2008;41:543–57.

[59] Wang Y-C, Hsu K. Shear strength of RC jacketed interior beam-column joints. ACI Struct J 2009;106(2):222–32.

[60] Yang H, Zhao W, Zhu Z, Fu J. Seismic behavior comparison of reinforced concrete interior beam-column joints based on different loading methods. Eng Struct 2018;166:31–45.